Wealth Mobility in the United States: Empirical Evidence from the PSID

Christophe Van Langenhove*

First Version: January 2025
This Version: April 2026

Abstract

U.S. wealth mobility is low and has declined across birth cohorts. I use the Panel Study of Income Dynamics (PSID) over 1969–2021 to measure inter-generational wealth mobility, intra-generational wealth mobility, and within-family wealth rank interdependence. Parent-child rank-rank coefficients range from 0.34 to 0.39 and rise with age. Over three generations, top persistence erodes faster than bottom persistence. Within generations, only 29% of individuals experience meaningful wealth rank mobility during working life. Most reshuffling occurs between ages 30 and 39. Children who rise within their birth cohort tend to have parents who also rise within theirs. Diverging wealth trajectories correlate with transfer receipts, business ownership, labor income, health, and non-mortgage debt. These moments provide calibration targets for heterogeneous agent models of the U.S. wealth distribution.

JEL classification: D14, D15, E21

Keywords: wealth mobility, wealth distribution, PSID, machine learning

*Vrije Universiteit Brussel (VUB) (email: christophe.van.langenhove@vub.be). I acknowledge the financial support from the Research Foundation Flanders (FWO, project 11I5324N). I am grateful to Arthur Apostel, Paula Gobbi, Freddy Heylen, David Johnson, Selma Malmberg, Marthe Mareels, Ive Marx, Yasin Kürşat Önder, Gert Peersman, Alberto Russo and Dirk Van de gaer for valuable comments, and to participants at the UGent internal seminar, ESPANet Early Career Researchers Day, 20th PSE Doctorissimes Conference, Inequalities & Opportunities Conference, 11th ECINEQ Conference, and ISI Wealth Conference 2025 for discussion and feedback.

1 Introduction

U.S. wealth mobility is low and has declined across birth cohorts. I use the Panel Study of Income Dynamics (PSID) over 1969–2021 to measure how wealth ranks transmit across generations, change within lifetimes, and co-move within families. Across generations, parent-child rank-rank coefficients range from 0.34 to 0.39. Over individual lifetimes, only 29% of individuals experience meaningful wealth rank mobility. Wealth persistence has risen across birth cohorts in both dimensions. Parents and children who move within their respective cohorts tend to move in the same direction.

Wealth inequality is well documented (Saez & Zucman, 2016; Smith et al., 2023), but wealth mobility is not. The same concentration of wealth can coexist with high or low wealth rank turnover at the top and bottom of the distribution. Without wealth mobility moments, heterogeneous agent models cannot be disciplined on this margin: stochastic returns, bequest motives, and earnings persistence all generate realistic wealth concentration, yet they differ in who stays wealthy and for how long[1]. I provide the missing wealth mobility moments along three dimensions.

First, I study inter-generational (family-level) wealth mobility. I compare individuals' wealth ranks within their birth cohort to those of their parents and grandparents. Parent-child rank-rank coefficients range from 0.34 to 0.39 for actual wealth. Wealth rank resemblance rises with age: proxy wealth coefficients increase by 31% from ages 30–34 to 60–64. Inter-generational wealth mobility has declined across recent cohorts: at prime working age (ages 40–44), the rank-rank coefficient rises by 45% between cohorts born around 1960 and those born in the late 1970s. Grandparent-grandchild coefficients are lower (0.20 to 0.22), with top persistence eroding faster than bottom persistence across three generations. U.S. inter-generational wealth mobility is low relative to most countries with available data.

[1]Models that generate realistic wealth concentration rely on stochastic returns (Benhabib et al., 2011; Gabaix et al., 2016), bequest motives (De Nardi, 2004), or both (De Nardi & Fella, 2017; Hubmer et al., 2021). These mechanisms have different implications for wealth mobility. Benhabib et al. (2019) calibrate to aggregate social mobility indices but not to the wealth mobility moments this paper provides.

Second, I study intra-generational (individual-level) wealth mobility. I track within-cohort wealth rank changes of individuals from ages 30 to 74. Only 29% of individuals exhibit meaningful wealth mobility during working life, lower than in most countries with available data. Most wealth rank reshuffling occurs between ages 30 and 39. Wealth positions crystallize further during older age. Intra-generational wealth mobility over ages 30–54 has declined across cohorts: the rank-rank coefficient β rises from 0.54 to 0.60 across cohort windows, an 11% increase. This decline is concentrated at the top, where persistence increases significantly.

Third, I bridge both perspectives by examining within-family wealth rank interdependence. Parents and children belong to different birth cohorts. I compare their wealth rank trajectories within their respective cohorts over the same calendar time. Children who rise within their cohort tend to have parents who also rise within theirs. Children who fall tend to have parents who fall. This interdependence is consistent with shared exposure to idiosyncratic risk (e.g. a family business or a shared local housing market) and grandparental transfers to both descendant generations.

Inter-generational wealth mobility Several papers study inter-generational wealth mobility in the United States using the PSID: Charles & Hurst (2003), Conley & Glauber (2008), Fisher & Johnson (2023), Mulligan (1997), and Pfeffer & Killewald (2018). Siminski & Yu (2022) study Australia using HILDA, with a PSID-based comparison. Menchik (1979) uses probate records. Among U.S. studies, only Pfeffer & Killewald (2018) extend the analysis to three generations.

Evidence for other countries is growing. Nordic studies include Adermon et al. (2018), Black et al. (2020), Boserup et al. (2017), and Fagereng et al. (2021). Gregg & Kanabar (2023) and Levell & Sturrock (2023) study the United Kingdom. Grabka et al. (2026) study Germany. Bourdieu et al. (2019) study historical France using probate records. Chu et al. (2024) use administrative records for Taiwan.

I make three contributions to this literature. First, I develop a gradient-boosting model to proxy wealth ranks before 1984, when the PSID did not record wealth. The model reduces the root mean squared rank prediction error by 32% relative to the best housing proxy (Pf-

effer & Killewald, 2018; Fisher & Johnson, 2023). Second, I extend the lifecycle analysis of Pfeffer & Killewald (2018) to all available stages and to three generations, documenting a new grandchild lifecycle bias. Third, I provide cross-country and cross-cohort comparisons that complement evidence from the Forbes 400 (Fernholz & Hagler, 2023) and align with results for Sweden (Adermon et al., 2018) and the United Kingdom (Gregg & Kanabar, 2023; Levell & Sturrock, 2023).

Intra-generational wealth mobility The intra-generational wealth mobility literature is relatively small. U.S. studies include Conley & Glauber (2008), Fisher et al. (2016), Jianakoplos & Menchik (1997), Klevmarken et al. (2003), Shiro et al. (2022), and Steckel & Krishnan (2006)[2]. Audoly et al. (2024) and Hubmer et al. (2024) study individual-level wealth mobility in Norway.

I contribute along three lines. First, I cover the full lifecycle from ages 30 to 74, separating working life and older age. Second, I document cross-cohort trends in intra-generational wealth mobility. Third, I characterize the sources of diverging wealth trajectories, linking them to intergenerational transfer receipts, business ownership, labor income, health, and non-mortgage debt.

Roadmap Section 2 introduces a framework for wealth mobility channels. Section 3 summarizes the data and methods. Sections 4–7 present the results. Section 8 concludes.

2 Wealth inequality & wealth mobility: framework & channels

2.1 Framework

Consider the following budget constraint for individual j:

$$w_j(t+1) = \left[1-\theta_j(t)\right]\left[w_j(t)(1+\alpha_j^a(t)r^a(t)+\alpha_j^i(t)r_j^i(t))+y_j(t)+m_j(t)+\mu_j(t)\right] \quad (1)$$

[2]Kuhn et al. (2020) and Kalsi & Ward (2025) include limited intra-generational analyses as robustness checks. A separate literature covers the Gilded Age (e.g. Dupont & Rosenbloom, 2022, Kearl & Pope, 1984, Steckel, 1990).

Here w_j denotes wealth and θ_j the consumption rate out of total resources. The terms α_j^a and r^a denote the allocation to and return on aggregate investment risk. The terms α_j^i and r_j^i denote the allocation to and return on idiosyncratic investment risk. The variables y_j, m_j, and μ_j denote labor income, net inter-generational transfer receipts, and household formation effects. I assume a zero riskless rate and abstract from taxation. A family consists of the individual, their parents, and their grandparents.

The behavioral variables θ_j, α_j^a, and α_j^i reflect both type and scale dependence. For any $z_j \in \{\theta_j, \alpha_j^a, \alpha_j^i\}$:

$$z_j(t) = \bar{z}\left[\kappa_j(t)\right] + \epsilon_j(t) \tag{2}$$

The term $\bar{z}[\kappa_j]$ captures scale dependence: parameter levels that vary with wealth rank κ_j. The term ϵ_j captures type dependence: structural parameter heterogeneity across individuals at identical wealth ranks[3].

Type dependence reflects ex-ante heterogeneity. Two individuals at near-identical wealth ranks may save or invest differently due to preferences, culture, or social norms. If persistent, these differences generate diverging wealth trajectories. Scale dependence reflects ex-post heterogeneity. After a positive shock (e.g. an inter-generational transfer receipt), an individual's wealth rank rises. This shock may trigger higher saving rates or aggregate risk allocations. Behavioral or institutional channels drive this response (e.g. superior investment fund access at higher wealth levels).

2.2 Wealth mobility channels

Equation 1 implies five channels of inter-generational transmission and four channels of intra-generational wealth mobility. I do not quantify their importance in this paper, but they serve as a framework for interpreting the results. Killewald et al. (2017), Lersch et al. (2024), and Elmelech (2026) provide complementary overviews.

[3] z_j may also vary over the lifecycle. I abstract from this for simplicity.

Inter-generational channels Five channels link parental wealth to children's wealth outcomes. First, parents transfer wealth directly through inter-vivos transfers and inheritances (Black et al., 2025). Second, parental wealth affects children's human capital and labor market outcomes through genetic, social, and network effects[4]. Third, high-return investments (housing, business) require upfront expenditures that parental wealth can finance (Lee et al., 2020). Fourth, children may inherit behavioral parameters (saving rates, risk-taking) from parents through genetic or social channels (Black et al., 2020; Davenport et al., 2021; Fagereng et al., 2021; Lindquist et al., 2015). Fifth, parental social networks influence household formation through assortative mating[5].

Intra-generational channels Four channels drive individual-level wealth mobility. First, diverging idiosyncratic risk realizations (labor income, business, housing) generate wealth mobility. Second, type dependence in behavioral parameters creates wealth mobility: individuals with dissimilar saving rates or risk allocations move relative to their wealth rank neighbors over time. Third, transfer receipts that differ across wealth rank neighbors generate relative wealth mobility. Fourth, household formation (partnership, marriage) reshuffles individuals across the wealth distribution.

Two features of the framework deserve emphasis. First, only type dependence generates wealth mobility. Scale dependence widens absolute wealth differences but does not change wealth ranks. Second, health operates as an additional channel that cuts across the four listed above (De Nardi et al., 2025; Mahler & Yum, 2024). Health shocks affect labor income, saving rates, and risk allocations. Health varies across individuals at the same wealth rank (type dependence) and wealth might enable access to better healthcare (scale dependence).

[4]See Holmberg et al. (2024), Karagiannaki (2017), Pfeffer (2018), and Staiger (2023).
[5]See Charles et al. (2013), Wagner et al. (2020), and Fagereng et al. (2022).

3 Data & methods

3.1 Data

I use the Panel Study of Income Dynamics (PSID). The PSID runs annually from 1968 to 1997 and biennially from 1999 to 2021. All waves record gross main housing values, mortgage debt, and rental payments. The waves in 1984, 1989, 1994, and 1999–2021 add questions on other assets and debts. I define wealth as total assets minus total debts. I refer to a full sample Ω (1969–2021) and a reduced sample Ψ (1984 onwards, where I observe wealth). Appendix A provides a detailed description.

I restrict the analysis to Survey Research Center (SRC) households and use unweighted estimates. The SRC subsample is an equal-probability sample by design, so weights correct only for differential non-response and attrition (Cooper et al., 2019). The rank transformation (see below) further reduces sensitivity to weighting: rank-based measures depend on the ordering of individuals, not on population-weighted totals. Pfeffer & Killewald (2018) use the full PSID sample with weights for inter-generational wealth mobility and report that unweighted results are similar.

3.2 Methodological contributions

I make two methodological contributions.

First, I harmonize and validate the PSID for wealth mobility research (Appendices A and C). The PSID underrepresents top wealth: average household wealth equals 44% of the Survey of Consumer Finances (SCF) average, and the top 10% wealth share is over 10 percentage points too low. This gap reflects a small number of missing ultra-wealthy households. Rank-based mobility metrics largely absorb this gap because they depend on household counts across the distribution, not on wealth levels, and the underestimation is time-invariant (Appendix A).

Second, I construct a gradient-boosting (GB) machine learning model to proxy wealth ranks before 1984 (Appendix D). Existing studies approximate pre-1984 wealth primarily from housing

values (Pfeffer & Killewald, 2018; Fisher & Johnson, 2023). My model incorporates additional socio-economic variables from the PSID and reduces the root mean squared rank prediction error by 32% relative to the best housing proxy. It misallocates 9% of households by more than 25 rank units per year, versus 21% for the best housing proxy.

3.3 Empirical strategy

The empirical strategy consists of three steps (Appendix E).

First, I allocate household wealth to individuals based on household status (equal split for married couples, income-proportional for unmarried partners, full assignment for singles)[6]. Second, I rank individuals within their ten-year birth cohort at each survey wave on a scale from 1 to 100. Within-cohort ranks avoid mechanical age effects and handle zero and negative wealth (Boserup et al., 2017). Third, I summarize each individual's ranks within five-year lifecycle stages (ages 30–34, 35–39, ..., 75+) by taking the median across survey waves. This aggregation smooths transitory measurement errors and is standard in the literature (Boserup et al., 2017; Gregg & Kanabar, 2023).

All results are reported for two wealth rank series: actual wealth ranks κ^{Ψ} (available from 1984, when the PSID first records wealth) and ML-proxied wealth ranks $\hat{\kappa}^{\Omega}$ (available from 1969). The proxy overstates wealth persistence in all analyses: the gap in β equals 0.03 to 0.05 for the inter-generational analysis (Section 4) and 0.10 for the intra-generational working life analysis (Section 5). This bias reflects the proxy model, not the difference in sample coverage: restricting the proxy to the post-1984 period ($\hat{\kappa}^{\Psi}$) produces the same results as the full-period proxy.

3.4 Outcome metrics

I use three types of wealth mobility metrics, moving from aggregate to granular. Appendix F provides formal definitions.

[6] Individuals may switch households over time. I therefore track individual wealth rank trajectories rather than household trajectories.

I measure overall wealth mobility using rank-rank coefficients β. I regress final within-cohort wealth ranks on initial wealth ranks using ordinary least squares (OLS). Higher β means higher wealth persistence and lower wealth mobility. The rank-rank coefficient is a descriptive measure of persistence, not a causal parameter. This approach is standard in the literature (Chetty et al., 2014; Deutscher & Mazumder, 2023; Mogstad & Torsvik, 2023).

To study wealth mobility at the bottom and top, I use transition probabilities and discretionary groups. Transition probabilities measure the chance of moving between wealth bins. For inter-generational analyses, the bins compare parents and children. For intra-generational analyses, the bins compare the same individual at two lifecycle stages. I report both ex-ante probabilities (conditioning on the starting bin) and ex-post probabilities (conditioning on the ending bin).

I also define six discretionary groups. Three capture the bottom: steady poor (start and end in the bottom 20%), past poor (start in the bottom 20%, rise to the top 50%), and new poor (start in the top 50%, fall to the bottom 20%). Three capture the top: steady wealthy (start and end in the top 10%), past wealthy (start in the top 10%, fall to the bottom 70%), and new wealthy (start in the bottom 70%, rise to the top 10%).

Hierarchical clusters group individuals by their full wealth rank trajectory over the lifecycle, following Audoly et al. (2024)[7]. Unlike discretionary groups, clusters cover every individual and reveal how broad-based wealth mobility is.

For rank-rank regressions, I cluster standard errors by family in inter-generational analyses (because multiple children share the same parent) and use heteroskedasticity-robust (HC1) standard errors in intra-generational analyses. For transition probabilities and discretionary group shares, I report 95% confidence intervals from a pairs bootstrap (100 replications). The bootstrap resamples families for inter-generational analyses and individuals for intra-generational analyses, preserving the relevant correlation structure.

[7] Hierarchical clustering applies only to the intra-generational analysis, which uses full trajectories as input. The Online Supplement provides a mathematical derivation of the algorithm.

Figure 1: Two-generational rank-rank coefficients β for parents and children at identical lifecycle stages for the pooled dataset.

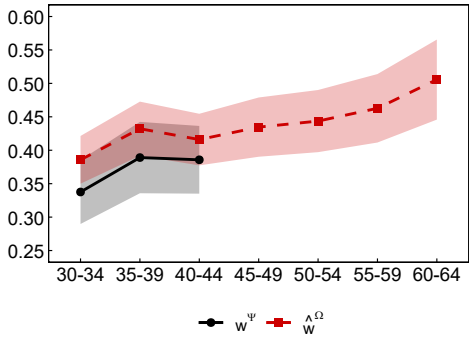

Note: OLS rank-rank coefficients β at identical lifecycle stages for the pooled dataset. Colors distinguish actual wealth ranks (κ^{Ψ}) and proxy wealth ranks ($\hat{\kappa}^{\Omega}$). Shaded ribbons show 95% family-clustered confidence intervals.

4 Inter-generational wealth mobility

This section compares wealth rank outcomes of individuals to those of their parents and grandparents. I restrict the sample to (grand)children's birth cohorts with at least 1,500 observations in one lifecycle stage combination. Appendix B reports sample sizes. The rank-rank regressions do not include age controls. Instead, I compute them across different lifecycle combinations to quantify the impact of age on the estimates.

4.1 Inter-generational wealth mobility across two generations

Children's wealth positions closely track those of their parents. The measured level of resemblance depends on age and measurement.

Rank-rank coefficients Parent-child rank-rank coefficients β range from 0.34 to 0.39 for actual wealth and from 0.39 to 0.51 for proxy wealth (Figure 1). Parent-child resemblance increases with age, peaking at ages 60–64: proxy wealth β is 31% higher than at ages 30–34. This upward-sloping β-profile reflects a parent-child lifecycle bias: the comparison age shapes the measured level of wealth persistence. Proxy wealth ranks overstate persistence by 0.03 to 0.05, approximately constant across lifecycle stages.

My estimates for actual wealth (0.34 to 0.39) align with existing PSID-based studies. Pfeffer & Killewald (2018) report 0.39, Siminski & Yu (2022) 0.31, and Fisher & Johnson (2023) 0.29 to 0.36. Earlier log-log specifications yield 0.28 to 0.37 (Charles & Hurst, 2003; Conley & Glauber, 2008).

The U.S. is among the least mobile countries. Several countries show lower persistence: β ranges from 0.17 to 0.25 in Norway (Fagereng et al., 2021; Audoly et al., 2024), equals 0.27 in Denmark (Boserup et al., 2017), 0.25 in Australia (Siminski & Yu, 2022), and 0.27 in Germany (Grabka et al., 2026). U.S. estimates are closer to those for the U.K. (0.30 to 0.36, Gregg & Kanabar, 2023; Levell & Sturrock, 2023), Sweden (0.30 to 0.39, Adermon et al., 2018; Black et al., 2020), and Taiwan (0.30 to 0.40, Chu et al., 2024)[8].

Lifecycle bias The lifecycle bias is well documented. Pfeffer & Killewald (2018) report β rising from 0.33 at ages 25–34 to 0.44 at ages 55–64 for the United States. Similar age gradients appear in Denmark (Boserup et al., 2017), Norway (Audoly et al., 2024), Sweden (Adermon et al., 2018), Australia (Siminski & Yu, 2022), and Taiwan (Chu et al., 2024).

Two patterns align with this bias. First, the share of transfer recipients rises substantially over working life (Van Langenhove, 2026). Rising transfer receipts are consistent with greater parent-child rank alignment over time (channel 1 in Section 2.2). Second, inherited labor market outcomes, type-dependent parameters, and assortative mating increasingly correlate with wealth outcomes as individuals age (channels 2–5 in Section 2.2).

Cross-cohort comparison Inter-generational wealth mobility has declined for recent birth cohorts (Figure 2). I track this decline using rolling ten-year birth cohort windows. At prime working age (ages 40–44), proxy wealth β rises by 45% between cohorts born around 1960 and those born in the late 1970s. The pattern holds at ages 35–39 through 50–54 and is confirmed by actual wealth. The wealth position a child is born into has become a stronger predictor of where that child ends up.

[8]These cross-country comparisons require caution. The estimates rely on different data sources (survey versus administrative records), wealth definitions, and lifecycle stages. The proxy-actual gap alone shifts β by 0.03 to 0.05, and comparing at different lifecycle stages introduces additional variation of similar or greater magnitude.

Figure 2: Rolling window rank-rank coefficients β for parents and children at identical life-cycle stages.

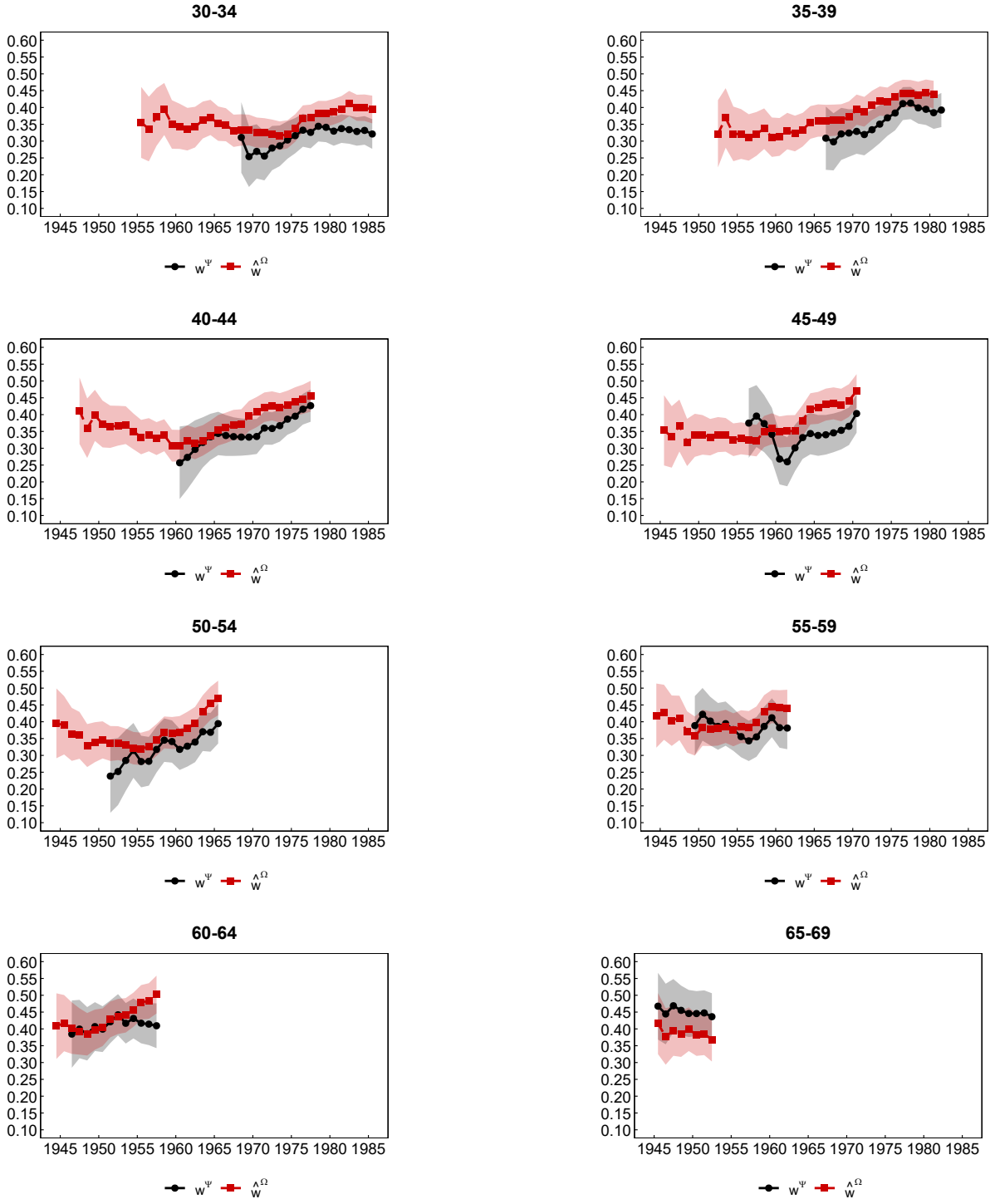

Note: OLS β from rolling ten-year birth cohort windows shifted by one year. Panel titles indicate lifecycle stages. Colors distinguish actual (κ^{Ψ}) and proxy ($\hat{\kappa}^{\Omega}$) wealth. Shaded ribbons show 95% family-clustered confidence intervals. Minimum 300 pairs per window.

Children from both poor and wealthy families are more likely to stay where they started than in earlier cohorts (Tables 10 and 11, Appendix G). Fernholz & Hagler (2023) report a similar pattern among the Forbes 400 since 1985. The decline also aligns with evidence for the U.K. (Gregg & Kanabar, 2023) and Sweden (Adermon et al., 2018).

Top versus bottom It is harder to leave the bottom of the wealth distribution than to stay at the top (Figure 3). At the bottom, 62% to 65% of children from bottom 50% parents remain in the bottom half. Upward mobility into the top 10% is rare (5%). The ex-post matrix confirms limited mixing (Figure 16, Appendix G). At the top, persistence is lower. Only 25% to 34% of children from top 10% parents stay in the top 10%, and 21% to 29% fall to the bottom half. Top 10% persistence also rises sharply with age, while bottom 50% persistence shows a weaker age gradient.

4.2 Inter-generational wealth mobility across three generations

Grandparent-grandchild wealth rank resemblance is weaker than the two-generational benchmark and exhibits a grandchild lifecycle bias.

Rank-rank coefficients For grandchildren aged 30–34, β ranges from 0.20 to 0.22 (actual wealth) and 0.25 to 0.31 (proxy wealth), which is well below the two-generational benchmark (Figure 4)[9]. A grandchild lifecycle bias appears: resemblance between grandchildren and grandparents is stronger when I observe grandchildren at ages 35–39 than at 30–34 (proxy wealth β is up to 7 points higher). Pfeffer & Killewald (2018) face the same bias because their grandchild sample is young. Boserup et al. (2014) find no such effect in Denmark, suggesting this bias is specific to the United States.

My actual wealth estimates (0.20 to 0.22) are close to Pfeffer & Killewald (2018), who report 0.23. The proxy estimates diverge. My ML proxy yields 0.25 to 0.31, above their housing value

[9]Data availability prevents comparing identical lifecycle stages across three generations: I observe grandparental wealth ranks from age 40 onwards and grandchild ranks only at ages 30–39 (in line with Boserup et al., 2014; Pfeffer & Killewald, 2018). I report two-generational outcomes over the same stage combinations (dotted lines) for comparison.

Figure 3: Ex-ante transition matrices $T_{\mathbf{EA}}(a)$ between parent and child wealth ranks at identical lifecycle stages for the pooled dataset.

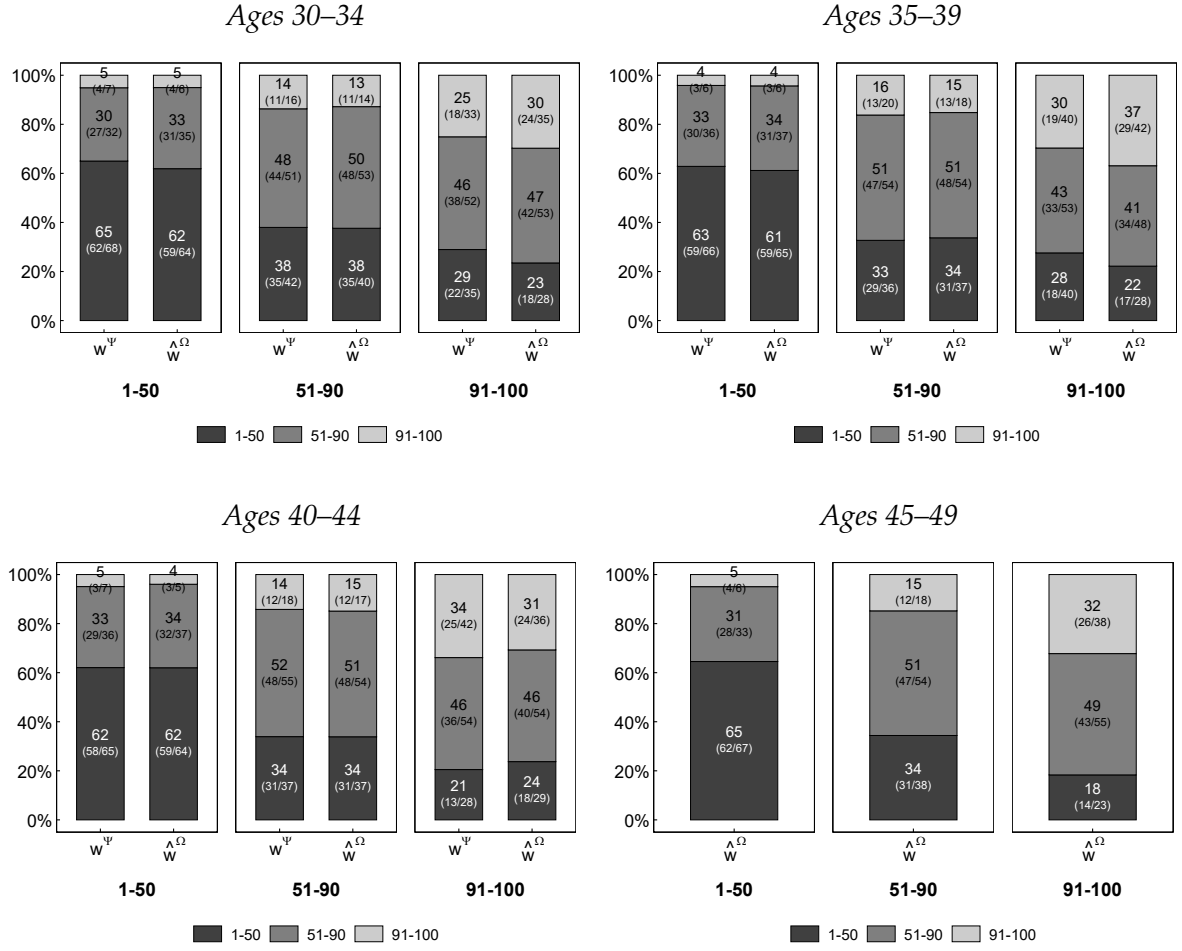

Note: Ex-ante matrices condition on parental wealth brackets (bottom 50%, middle 50–90%, top 10%). Stacked bars show the probability of children reaching each destination bracket. Columns within each panel distinguish actual wealth ranks (κ^{Ψ}) and proxy wealth ranks ($\hat{\kappa}^{\Omega}$). Numbers report transition probabilities (%). Parentheses show 95% bootstrapped confidence intervals (100 replications). Pooled dataset. Appendix G reports stages 50–54 and 55–59.

Figure 4: Rank-rank coefficients β for grandparents and grandchildren (solid lines) and parents and children (dotted lines) when (grand)children are aged 30–34 and 35–39.

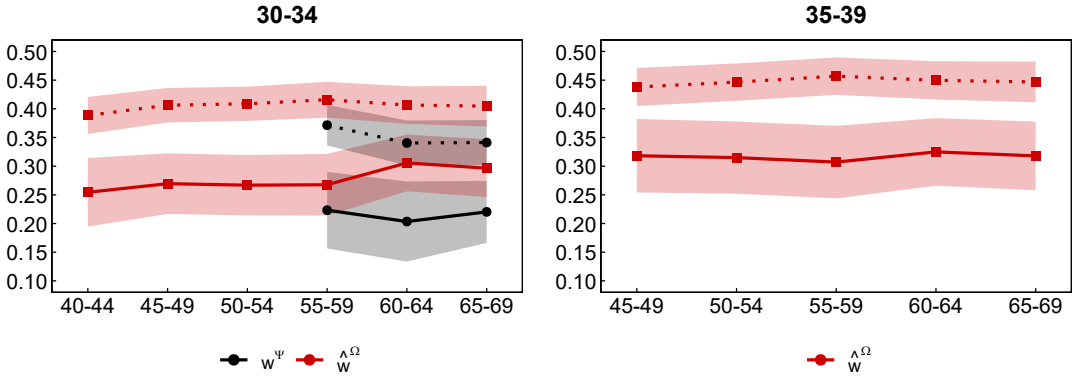

Note: Solid lines show grandparent-grandchild β, dotted lines show parent-child β (benchmark). Left panel covers (grand)children aged 30–34, right panel 35–39. Colors distinguish actual wealth ranks (κ^{Ψ}) and proxy wealth ranks ($\hat{\kappa}^{\Omega}$). Shaded ribbons show 95% family-clustered confidence intervals. Pooled dataset.

proxy estimate of 0.21. The housing proxy likely understates persistence during the post-2008 years, when housing values were a poorer predictor of total wealth (Appendix D).

Three-generational persistence is also higher in the U.S. than in Denmark ($\beta = 0.16$, Boserup et al., 2014) and Sweden (0.14 to 0.17, Adermon et al., 2018). Because the grandchild lifecycle bias is specific to the U.S., this gap likely widens when grandchildren are observed at later ages.

Top versus bottom Bottom wealth positions endure across three generations. Top positions erode (Figure 5). I report actual wealth for grandchildren aged 30–34. Proxy wealth produces qualitatively similar patterns.

At the bottom, three-generational persistence is close to two-generational persistence. Grandchildren from bottom 20% grandparents still face a 24% chance of remaining in the bottom 20%, compared to 33%–36% over two generations. At the top, persistence drops sharply. Only 14%–18% of grandchildren from top 10% grandparents remain in the top 10%, down from 27%–33% over two generations. This pattern also holds at grandchild stage 35–39 (Figure 18, Appendix G).

Figure 5: Transition probabilities for grandparents and grandchildren (solid lines) and parents and children (dotted lines) when (grand)children are aged 30–34.

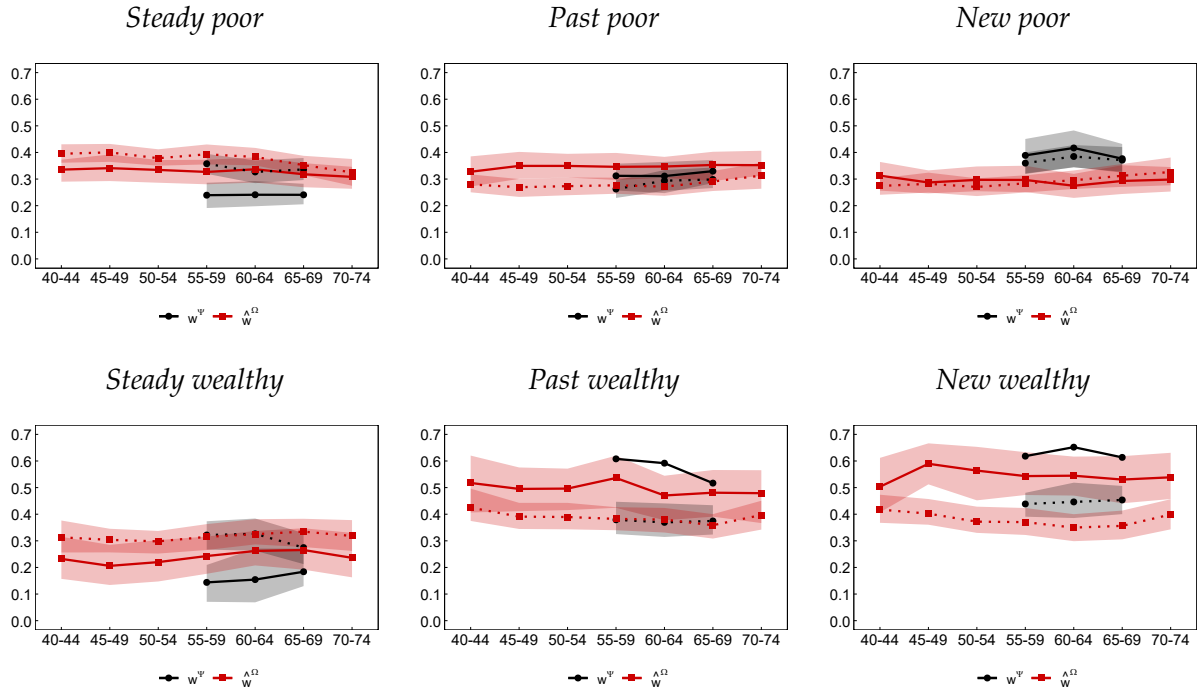

Note: Each subplot shows one discretionary group (see Section 3.4). (Grand)children fixed at ages 30–34. The horizontal axis varies (grand)parental stage. Solid lines show grandparent-grandchild, dotted lines show parent-child. Colors distinguish wealth rank measures (κ^{Ψ}, $\hat{\kappa}^{\Omega}$). Shaded ribbons show 95% bootstrapped confidence intervals (100 replications). Appendix G reports stage 35–39.

Two features of the data help explain why top persistence erodes faster. First, inter-generational transfers are small relative to lifetime resources. Even for steady wealthy families, cumulative receipts average only 10% of lifetime resources at the start of working life[10]. Direct monetary transfers are therefore too small to mechanically reproduce wealth persistence across three generations (see also Van Langenhove, 2026). Second, wealthy families disproportionately own businesses (Online Supplement), which carry high idiosyncratic risk and are a plausible mechanism for faster erosion of top positions over longer horizons[11]. At the bottom, by contrast, families remain in multi-generational low-wealth positions associated with low income, poor health, and negligible transfers (Online Supplement).

5 Intra-generational wealth mobility

I track how individual wealth positions evolve over the lifecycle, studying within-cohort wealth inequality and mobility for working life (ages 30–54) and older age (ages 55–74). I restrict the sample to balanced panels: each individual appears at both the start and end of each phase. I keep only birth cohorts with at least 250 individuals. Appendix B reports sample sizes.

Attrition is differential by wealth. For working life, retention equals 54% among bottom 50% individuals and 60% among the top 10% (Appendix B.3). The estimated β is therefore an upper bound on true persistence.

5.1 Within-cohort inequality and initial conditions

Within-cohort wealth inequality is high and stable over the lifecycle (Figure 6). The top 10% hold 55% to 60% of within-cohort wealth during working life. The bottom 50% own 3% to 5%. These shares track the SCF estimates of Bauluz & Meyer (2024), change little across lifecycle stages, and are stable in relative terms despite large differences in absolute wealth growth

[10] Towards the end of working life, this fraction is higher for the wealthiest individuals (31%). Black et al. (2025) find similar magnitudes for Norway. Van Langenhove (2026) documents similar patterns for the United States.

[11] Kalsi & Ward (2025) find low persistence among the wealthiest during the U.S. Gilded Age and attribute it to entrepreneurial luck and skill, neither of which parents reliably pass on to their children.

Figure 6: Wealth shares λ_b across lifecycle stages by birth cohort, based on actual wealth levels w^{Ψ}.

Working life (ages 30–54)

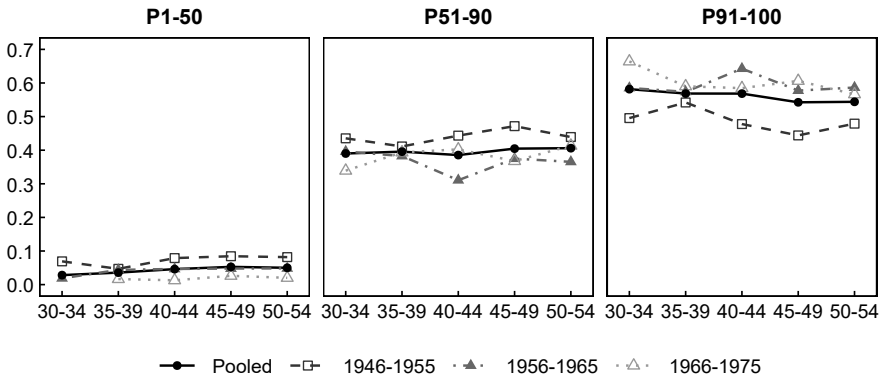

Older age (ages 55–74)

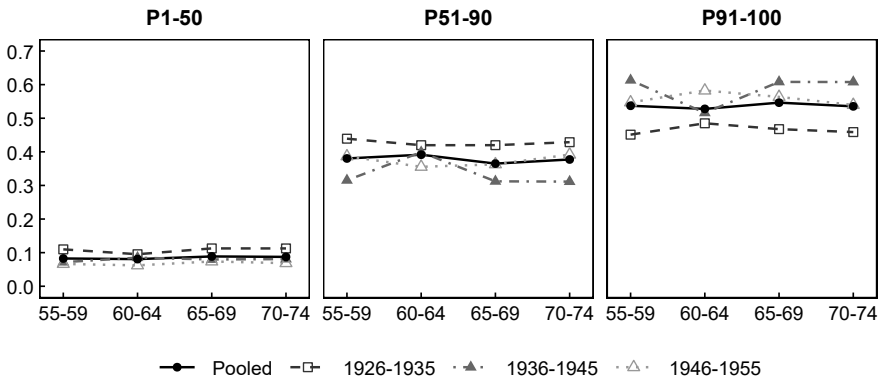

Note: Each sub-panel shows the fraction of within-cohort wealth held by one bracket (P1–50, P51–90, P91–100) across lifecycle stages, by birth cohort. Actual wealth w^{Ψ}. Working life and older age samples contain different individuals.

Table 1: Pooled rank-rank coefficients β for intra-generational wealth mobility.

	Actual κ^{Ψ}	Proxy $\hat{\kappa}^{\Omega}$
Working life (ages 30–54)	0.57	0.67
	(0.02)	(0.01)
Older age (ages 55–74)	0.77	0.80
	(0.02)	(0.01)

Note: OLS β with HC1 standard errors in parentheses. Working life compares ages 30–34 to 50–54. Older age compares ages 55–59 to 70–74. Appendix B reports sample sizes.

across brackets[12]. Within-cohort inequality has increased across birth cohorts: the 1966–75 cohort enters working life with a top 10% share of 66%, far above earlier cohorts, and bottom 50% shares in recent cohorts lie closer to zero (Bauluz & Meyer, 2024).

Initial wealth positions already reflect family background. Most individuals start working life with little wealth: 53% have wealth below annual labor income at ages 30–34 (Figure 20, Appendix G). Those who start wealthy disproportionately come from wealthy families: 21% of top 10% individuals at ages 30–34 have parents in the parental top 10%, over twice the random benchmark of 10% (Section 4). Inter-generational transfers reinforce this overlap: 31% of top 10% individuals have received a transfer by ages 30–34, versus 16% of bottom 50% individuals. Boserup et al. (2018) find a similar pattern in Denmark at age 18.

5.2 Wealth mobility during working life

Stable within-cohort inequality does not imply fixed wealth positions. I now examine individual-level rank changes over working life (ages 30–54).

Rank-rank coefficients The pooled rank-rank coefficient between ages 30–34 and 50–54 equals 0.57 (Table 1). Proxy wealth ranks overstate persistence ($\hat{\kappa}^{\Omega}$: 0.67 versus κ^{Ψ}: 0.57). My estimate aligns with Shiro et al. (2022), who report 0.59 for the U.S. over a similar age span, and with the log-log correlation of 0.47 in Conley & Glauber (2008). U.S. intra-generational

[12]Wealth-to-income ratios increase roughly 2-fold for the top 10% and 12-fold for the bottom 50% during working life, reflecting differences in starting levels (Appendix G).

Figure 7: Ex-ante transition matrices $T_{\mathbf{EA}}(a)$ during working life and older age for the pooled dataset.

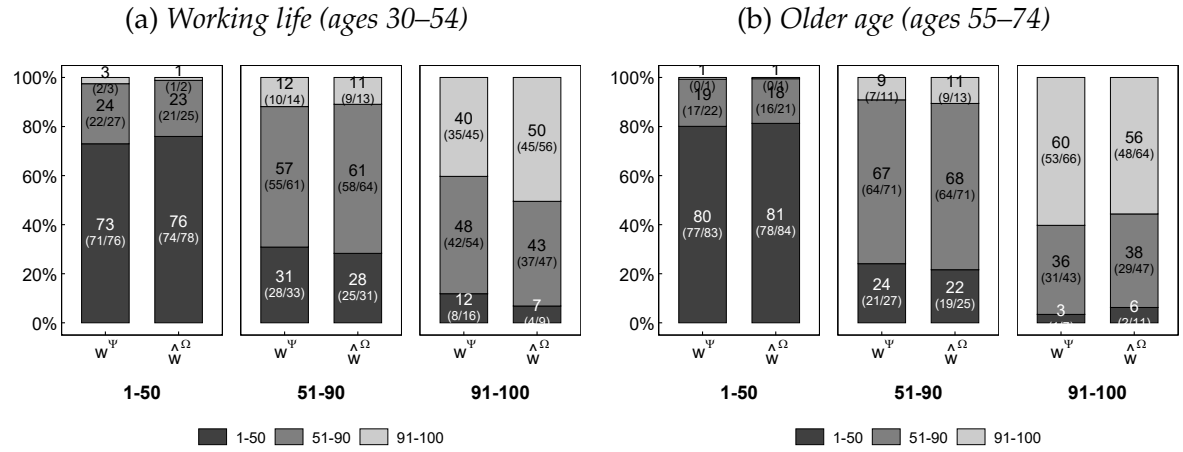

Note: Ex-ante matrices condition on initial wealth brackets (bottom 50%, middle 50–90%, top 10%). Left panel shows actual wealth ranks (κ^{Ψ}), ages 30–34 vs. 50–54. Right panel shows ages 55–59 vs. 70–74. Numbers report transition probabilities (%). Parentheses show 95% bootstrapped confidence intervals (100 replications). Appendix G reports ex-post matrices.

wealth mobility is lower than in most countries with available data: $\beta = 0.20$ in Norway (Audoly et al., 2024) and 0.26 in Denmark (Boserup et al., 2018).

Top versus bottom It is harder to escape the bottom than to fall from the top (Figure 7, panel a). I report actual wealth. Proxy wealth produces similar patterns with higher persistence. At the bottom, 73% of bottom 50% individuals at ages 30–34 remain there by ages 50–54, and only 3% reach the top 10%. At the top, only 40% of the top 10% at ages 30–34 remain there by ages 50–54, consistent with the 64% top-quintile persistence over 14 years reported by Fisher et al. (2016). The top 10% at ages 50–54 is not a closed group: 60% of its members started in the bottom 70% (Figure 21, Appendix G).

Hierarchical clustering confirms this picture (Figure 8, panel a). The algorithm groups individuals by the shape of their full wealth rank trajectory and assigns each to one of four categories: bottom, middle, top, or mobile (Appendix F). Most individuals do not move. 39% belong to bottom clusters, 11% to middle clusters, and 21% to top clusters. Only 29% belong to mobile clusters. This mobile share is well below the 40% reported for Norway (Audoly et al., 2024).

Figure 8: Average within-cohort wealth rank trajectories by hierarchical cluster (κ^{Ψ}), pooled dataset.

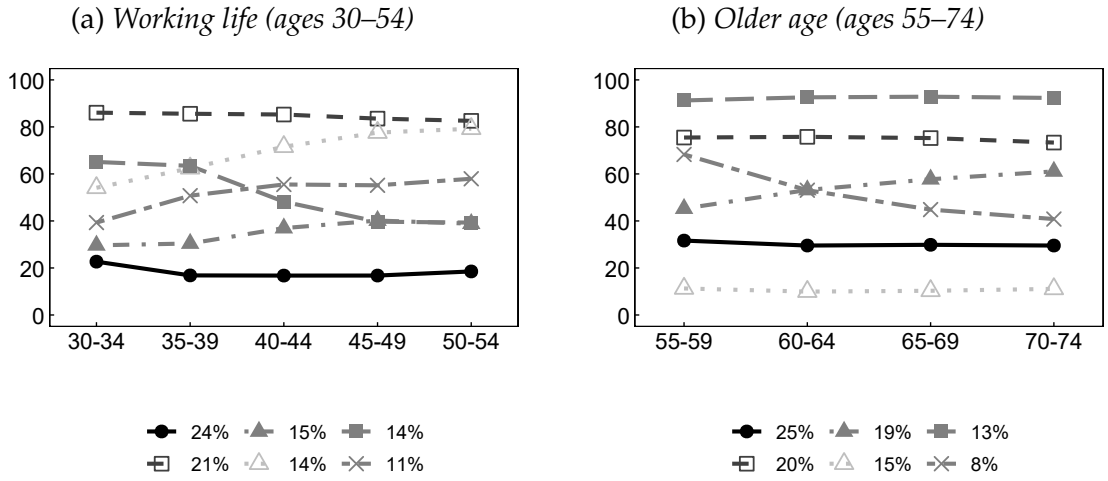

Note: Six hierarchical clusters of individual wealth rank trajectories (κ^{Ψ}). Legend reports cluster shares. Clusters are classified as mobile (trajectory range $>$ 20 rank points), bottom (average rank $\leq$ 40), middle (40–80), or top ($\geq$ 80); see Appendix F. Clustering algorithm in the Online Supplement, which also reports proxy wealth results.

5.3 Wealth mobility during older age

Rank-rank coefficients Wealth positions crystallize during older age (ages 55–74). The pooled rank-rank coefficient between ages 55–59 and 70–74 equals 0.77, versus 0.57 for working life. The shorter time span does not drive this gap. Rank-rank coefficients for 20-year working life windows also fall below older-age levels (0.62 for ages 30–49, 0.68 for ages 35–54).

Differential mortality likely biases this estimate: the sample includes only individuals alive at ages 70–74. Individuals who die earlier may experience downward wealth mobility from health shocks that the balanced panel does not capture. The coefficient of 0.77 therefore likely understates actual older-age wealth mobility.

Top versus bottom Persistence is high at both tails (Figure 7, panel b). At the bottom, 80% of bottom 50% individuals at ages 55–59 remain there by ages 70–74. Upward wealth mobility into the top 10% is near zero (1%). At the top, 60% of top 10% individuals remain by ages 70–74, with only 3% dropping to the bottom 50%. Hierarchical clustering confirms these patterns

(Figure 8, panel b). Applying the same classification as for working life (Appendix F), 40% of individuals belong to bottom clusters, 39% to middle clusters, 13% to top clusters, and 8% to mobile clusters. Unlike working life, the mobile clusters during older age are predominantly downward, consistent with health-driven wealth decumulation.

5.4 Timing effects

Most wealth mobility occurs early in working life. Figure 9 presents rank-rank coefficients from a rolling window analysis. The β-estimate for the 30–34 to 35–39 transition equals 0.72. Later working-life transitions produce higher coefficients (0.80 to 0.84), and older-age transitions are higher still (0.87 to 0.90). Wealth ranks become increasingly sticky with age. Cluster trajectories confirm the pattern: mobile clusters show most movement before age 40 (Figure 8, panel a). Audoly et al. (2024) find similar timing effects for Norway.

This concentration of wealth mobility early in working life holds at both tails (Figures 22 and 23, Appendix G)[13]. At the bottom, the probability that a bottom 20% individual remains there in the next stage rises from 55% (ages 30–34 to 35–39) to 67% (ages 45–49 to 50–54). At the top, the probability that a top 10% individual remains there rises from 55% to 72% over the same transitions. Wealth ranks lock in progressively: the window for rank mobility narrows after age 40.

Three features of the data align with early concentration of wealth mobility. First, absolute wealth differences are smallest at the start (Section 5.1). Additive shocks (labor income, intergenerational transfers, household formation) therefore generate larger wealth rank changes. Second, idiosyncratic risk-taking peaks between ages 30 and 39, as reflected in higher business portfolio shares (Online Supplement). Third, equity and housing participation is lowest at the start of working life, meaning that wealth rank neighbors might face different aggregate risk exposures (Figure 26, Appendix H).

[13] These patterns are more pronounced when I use age group 25–29 as the starting point, as shown in the Online Supplement.

Figure 9: Rank-rank coefficient β between consecutive lifecycle stages, working life and older age.

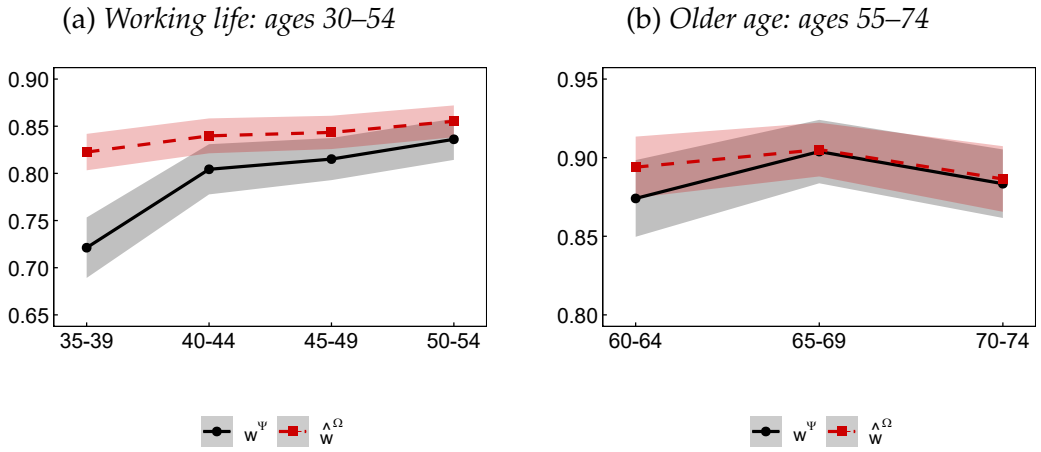

Note: OLS β between consecutive lifecycle stages. Colors distinguish actual wealth (κ^{Ψ}) and proxy wealth ($\hat{\kappa}^{\Omega}$). Shaded ribbons show 95% HC1 confidence intervals.

5.5 Cross-cohort comparison

Intra-generational wealth mobility has declined across birth cohorts. β rises from 0.54 for the earliest cohorts to 0.60 for the most recent, an 11% increase (Figure 10). The trend is gradual: each successive cohort shows equal or higher persistence. This aggregate trend conceals a sharp divergence between top and bottom.

The decline is concentrated at the top. The steady wealthy share rises from 30% to 46% across cohorts. Fewer outsiders break in: the new wealthy share falls from 14% to 7% (Figure 25, Appendix G). The top 10% is becoming a more closed group. At the bottom, the steady poor share declines from 46% to 38%, but the change is smaller than at the top. The decline in intra-generational wealth mobility is driven entirely by the top of the distribution.

6 Within-family wealth rank interdependence

I bridge the inter-generational and intra-generational perspectives by examining whether parent and child wealth rank trajectories are interdependent over the same calendar time. Parents and children belong to different birth cohorts, so their wealth ranks are computed within

Figure 10: Rolling window analysis across birth cohorts, working life (ages 30–54).

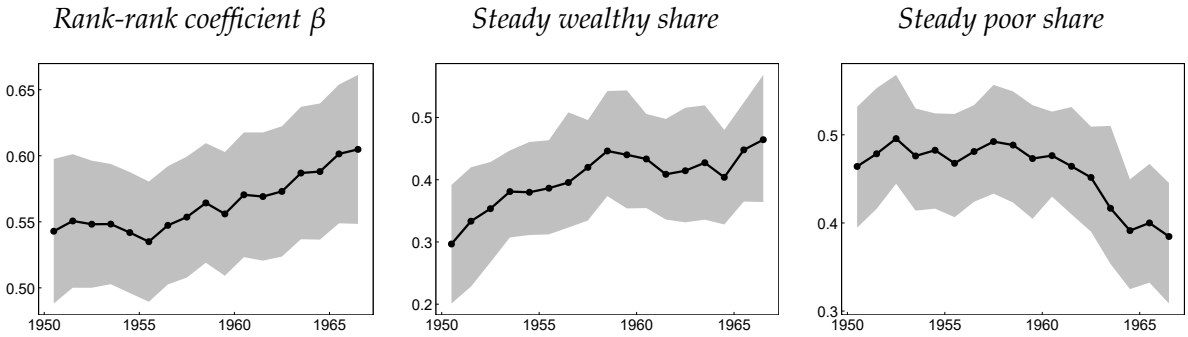

Note: Rolling ten-year birth cohort windows shifted by one year. Left panel shows the rank-rank coefficient β (ages 30–34 to 50–54). Middle and right panels show transition probabilities: the steady wealthy share (probability of starting and ending in the top 10%) and the steady poor share (probability of starting and ending in the bottom 20%). Actual wealth ranks (κ^{Ψ}). Shaded ribbons show 95% confidence intervals (HC1 for β, bootstrapped for shares with 100 replications). Minimum 300 individuals per window.

separate cohort distributions. Appendix B reports sample sizes. I classify children into discretionary groups based on their intra-generational trajectory (Section 5) and track the fraction whose parents rank in the top 10% or top 30% of the parental cohort at each lifecycle stage (Figure 11).

Parent-child co-movement Parent and child wealth ranks are interdependent: when a child rises within their cohort, the parent tends to rise within theirs. When a child falls, the parent tends to fall. Three patterns emerge.

First, children who rise from the bottom 20% to the top half of their cohort (past poor) increasingly have parents in strong parental positions. The fraction with parents in the parental top 10% rises from 12% to 21% over working life. The parents of upwardly mobile children are themselves rising within the parental cohort. Second, children who fall from the top 10% to the bottom 70% (past wealthy) increasingly have parents in weaker positions. The fraction with parents in the parental top 10% drops from 15% to 7%. The parents of downwardly mobile children are themselves falling. Third, children with stable positions have parents with stable positions. For steady wealthy children, 71% have parents in the parental top 30% throughout. For steady poor children, only 9% to 13% do.

Figure 11: Fraction of individuals with parents in the top 10% or top 30% of the parental wealth distribution, by discretionary group (κ^{Ψ}).

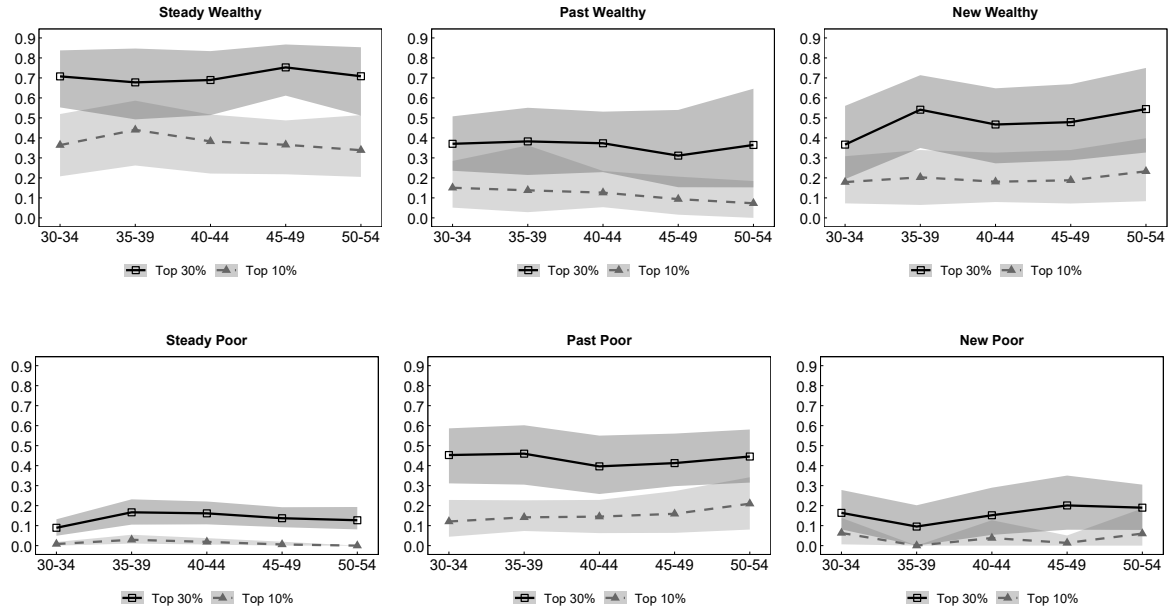

Note: Each subplot shows one discretionary group. Lines report the fraction of individuals whose parents rank in the top 10% or top 30% of the parental within-cohort distribution at each lifecycle stage. Shaded ribbons show 95% bootstrapped confidence intervals (100 replications). Working life sample. Individuals without parental observations are excluded.

What drives the interdependence? Two channels are consistent with this interdependence (Section 2.2). First, shared exposure to idiosyncratic risk: parents and children who participate in the same family business, own property in the same housing market, or live in the same region face correlated shocks that push both up or down within their respective cohorts. Second, grandparental transfers: if grandparents transfer wealth to both parents and children simultaneously, both rise within their cohorts. Direct parent-to-child transfers alone cannot explain the interdependence, because they raise the child's rank but lower the parent's.

7 Sources of wealth mobility

What distinguishes diverging wealth trajectories? I compare inter-generational transfer receipts and socio-economic characteristics across the discretionary groups and clusters from Section 5. The analysis is descriptive, not causal (Section 2.2). I use the intra-generational working life sample. The Online Supplement shows that the findings extend to family-level wealth mobility[14]. Appendix H.1 defines all composition metrics. Two findings stand out (Figure 27, Appendix H). The Online Supplement reports the same metrics for hierarchical clusters.

First, transfer receipts are far more common among the steady wealthy (66% by ages 50–54) than the steady poor (55%), but even for the wealthiest, cumulative receipts constitute only 31% of lifetime resources[15]. Transfers correlate with top persistence but are too small to mechanically explain it. This limited direct role aligns with U.S. evidence (Charles & Hurst, 2003; Pfeffer & Killewald, 2018; Van Langenhove, 2026) and Norwegian evidence (Audoly et al., 2024). Sabelhaus (2024) estimates that indirect channels (education, risk tolerance, business startup, and income) account for roughly 60% of the inter-generational wealth rank correlation, with direct transfers explaining the remainder.

[14] See Adermon et al. (2021), Charles & Hurst (2003), Fagereng et al. (2021), and Lindquist et al. (2015). König et al. (2025) and Hubmer et al. (2024) study the very top (top 1% and beyond).

[15] Lifetime resources equal 35 times average annual labor income, capitalized to the terminal year. Unlike Black et al. (2025), I exclude government transfers. The exclusion may bias the ratio upward for poorer individuals.

Second, labor income is the strongest correlate of wealth persistence. Steady wealthy individuals consistently rank in the top 40% of the income distribution. Bottom persistence and downward mobility correlate with low and declining labor income. Charles & Hurst (2003) find that lifetime income and asset ownership jointly explain nearly two-thirds of the inter-generational wealth elasticity. Audoly et al. (2024) find human capital to be the main predictor for Norway. Davenport et al. (2021) find that education and earnings account for roughly half of inter-generational wealth persistence in the United Kingdom.

Three further correlates emerge. Business ownership correlates with both top consolidation and downward mobility, though the link with upward mobility is inconclusive (Audoly et al., 2024, find a similar pattern for Norway). Wealthy individuals have higher equity and home-ownership rates, though they allocate a smaller share of their portfolio to housing. Bottom persistence and downward mobility correlate with poor health, single-headed household status, and elevated non-mortgage indebtedness.

8 Conclusion

I use the PSID to document inter-generational wealth mobility, intra-generational wealth mobility, and within-family wealth rank interdependence in the United States over 1969–2021.

Three findings stand out. First, U.S. wealth mobility is low relative to most countries with available data, both across and within generations. Parent-child rank-rank coefficients range from 0.34 to 0.39. Intra-generational persistence equals $\beta = 0.57$ over working life and $\beta = 0.77$ over older age. Second, wealth mobility has declined across birth cohorts. Inter-generational persistence has risen significantly at prime working age. Intra-generational persistence over working life has also increased, concentrated at the top of the distribution where changes are statistically significant. Third, wealth rank trajectories of parents and children are interdependent within their respective cohorts: children who rise tend to have parents who also rise.

These moments discipline heterogeneous agent models of U.S. wealth dynamics. Matching the cross-sectional wealth distribution is not enough: different models can produce the same dis-

tribution through very different underlying dynamics. For instance, a bequest-driven model predicts a jump in parent-child resemblance around inheritance age. An earnings-persistence model predicts a gradual rise. The lifecycle profiles I estimate distinguish between these mechanisms.

References

Adermon, A., Lindahl, M., Waldenström, D. (2018). Intergenerational Wealth Mobility and the Role of Inheritance: Evidence from Multiple Generations. *The Economic Journal* 128 (612), pp. F482–F513.

Adermon, A., Lindahl, M., Palme, M. (2021). Dynastic Human Capital, Inequality, and Intergenerational Mobility. *American Economic Review* 111 (5), pp. 1523–1548.

Audoly, R., McGee, R., Ocampo, S., Paz-Pardo, G. (2024). The Life-Cycle Dynamics of Wealth Mobility. Federal Reserve Bank of New York Staff Reports, no. 1097.

Bauluz, L., Meyer, T. (2024). The Wealth of Generations. Available at SSRN 3834260.

Benhabib, J., Bisin, A., Zhu, S. (2011). The Distribution of Wealth and Fiscal Policy in Economies with Finitely Lived Agents. *Econometrica* 79 (1), pp. 123–157.

Benhabib, J., Bisin, A., Luo, M. (2019). Wealth Distribution and Social Mobility in the US: A Quantitative Approach. *American Economic Review* 109 (5), pp. 1623–1647.

Black, S., Devereux, P., Lundborg, P., Majlesi, K. (2020). Poor Little Rich Kids? The Role of Nature versus Nurture in Wealth and Other Economic Outcomes and Behaviours. *The Review of Economic Studies* 87 (4), pp. 1683–1725.

Black, S., Devereux, P., Landaud, F., Salvanes, K. (2025). The (un)Importance of Inheritance. *Journal of the European Economic Association* 23 (3), pp. 1060–1094.

Boserup, S., Kopczuk, W., Kreiner, C. (2014). Stability and Persistence of Intergenerational Wealth Formation: Evidence from Danish Wealth Records of Three Generations. Unpublished.

Boserup, S., Kopczuk, W., Kreiner, C. (2017). Intergenerational Wealth Formation over the Life Cycle: Evidence from Danish Wealth Records 1984–2013. Unpublished.

Boserup, S., Kopczuk, W., Kreiner, C. (2018). Born with a Silver Spoon? Danish Evidence on Wealth Inequality in Childhood. *The Economic Journal* 128 (612), pp. F514–F544.

Bourdieu, J., Kesztenbaum, L., Postel-Vinay, G., Suwa-Eisenmann, A. (2019). Intergenerational Wealth Mobility in France, 19th and 20th Century. *Review of Income and Wealth* 65 (1), pp. 21–47.

Charles, K., Hurst, E. (2003). The Correlation of Wealth across Generations. *Journal of Political Economy* 111 (6), pp. 1155–1182.

Charles, K., Hurst, E., Killewald, A. (2013). Marital Sorting and Parental Wealth. *Demography* 50, pp. 51–70.

Chetty, R., Hendren, N., Kline, P., Saez, E. (2014). Where is the Land of Opportunity? The Geography of Intergenerational Mobility in the United States. *The Quarterly Journal of Economics* 129 (4), pp. 1553–1623.

Chu, Y.W.L., Lin, M.J., Nian, H. (2024). The Apple Doesn't Fall Far from the Tree: Intergenerational Wealth Mobility in Taiwan. *Labour Economics* 91, 102617.

Conley, D., Glauber, R. (2008). Wealth Mobility and Volatility in Black and White. Washington, DC: Center for American Progress.

Cooper, D., Dynan, K., Rhodenhiser, H. (2019). Measuring Household Wealth in the Panel Study of Income Dynamics: The Role of Retirement Assets. Working Papers No. 19-6, Federal Reserve Bank of Boston, Boston, MA.

Davenport, A., Levell, P., Sturrock, D. (2021). Why Do Wealthy Parents Have Wealthy Children? IFS Report No. R196, Institute for Fiscal Studies.

De Nardi, M. (2004). Wealth Inequality and Intergenerational Links. *The Review of Economic Studies* 71 (3), pp. 743–768.

De Nardi, M., Fella, G. (2017). Saving and Wealth Inequality. *Review of Economic Dynamics* 26, pp. 280–300.

De Nardi, M., Pashchenko, S., Porapakkarm, P. (2025). The Lifetime Costs of Bad Health. *The Review of Economic Studies* 92 (3), pp. 1987–2026.

Deutscher, N., Mazumder, B. (2023). Measuring Intergenerational Income Mobility: A Synthesis of Approaches. *Journal of Economic Literature* 61 (3), pp. 988–1036.

Dupont, B., Rosenbloom, J.L. (2022). Wealth Mobility in the United States: 1860–1870. *Social Science History* 46 (4), pp. 801–829.

Elmelech, Y. (2026). Wealth Mobility and Inequality: A Theoretical Framework. *Social Science Research*, 103278.

Fagereng, A., Mogstad, M., Rønning, M. (2021). Why Do Wealthy Parents Have Wealthy Children? *Journal of Political Economy* 129 (3), pp. 703–756.

Fagereng, A., Guiso, L., Pistaferri, L. (2022). Assortative Mating and Wealth Inequality. National Bureau of Economic Research Working Paper No. 29903.

Fernholz, R., Hagler, K. (2023). Rising Inequality and Declining Mobility in the Forbes 400. *Economics Letters* 230, 111235.

Fisher, J., Johnson, D., Latner, J.P., Smeeding, T., Thompson, J. (2016). Inequality and Mobility Using Income, Consumption, and Wealth for the Same Individuals. *RSF: The Russell Sage Foundation Journal of the Social Sciences* 2 (6), pp. 44–58.

Fisher, J., Johnson, D. (2023). Intergenerational Mobility using Income, Consumption and Wealth. Washington Center for Equitable Growth Working Paper No. 060723.

Gabaix, X., Lasry, J.-M., Lions, P.-L., Moll, B. (2016). The Dynamics of Inequality. *Econometrica* 84 (6), pp. 2071–2111.

Grabka, M., Lersch, P., Longmuir, M., Schnitzlein, D. (2026). Intergenerational Wealth Mobility in Germany. Unpublished.

Gregg, P., Kanabar, R. (2023). Intergenerational Wealth Transmission in Great Britain. *Review of Income and Wealth* 69 (4), pp. 807–837.

Heathcote, J., Storesletten, K., Violante, G. (2010). The Macroeconomic Implications of Rising Wage Inequality in the United States. *Journal of Political Economy* 118 (4), pp. 681–722.

Holmberg, J., Simmons, M., Trapeznikova, I. (2024). Parental Wealth and Early Labor Market Outcomes. Unpublished.

Hubmer, J., Krusell, P., Smith, A. (2021). Sources of U.S. Wealth Inequality: Past, Present and Future. *NBER Macroeconomics Annual* 35 (1), pp. 391–455.

Hubmer, J., Halvorsen, E., Salgado, S., Ozkan, S. (2024). Why Are the Wealthiest So Wealthy? New Longitudinal Empirical Evidence and Implications for Theories of Wealth Inequality. Federal Reserve Bank of St. Louis Working Paper 2024-013.

Insolera, N., Simmert, B., Johnson, D. (2021). An Overview of Data Comparisons Between PSID and Other U.S. Household Surveys. Panel Study of Income Dynamics Technical Series Paper #21-02.

Jianakoplos, N., Menchik, P. (1997). Wealth Mobility. *The Review of Economics and Statistics* 79 (1), pp. 18–31.

Jordà, O., Knoll, K., Kuvshinov, D., Schularick, M., Taylor, A. (2019). The Rate of Return on Everything, 1870–2015. *The Quarterly Journal of Economics* 134 (3), pp. 1225–1298.

Kalsi, P., Ward, Z. (2025). The Gilded Age and Beyond: The Persistence of Elite Wealth in American History. NBER Working Paper No. 33355.

Kaplan, G., Violante, G., Weidner, J. (2014). The Wealthy Hand-to-Mouth. *Brookings Papers on Economic Activity* 2014 (1), pp. 77–138.

Karagiannaki, E. (2017). The Effect of Parental Wealth on Children's Outcomes in Early Adulthood. *The Journal of Economic Inequality* 15 (3), pp. 217–243.

Kearl, J., Pope, C. (1984). Mobility and Distribution. *The Review of Economics and Statistics* 66, pp. 192–199.

Killewald, A., Pfeffer, F., Schachner, J. (2017). Wealth Inequality and Accumulation. *Annual Review of Sociology* 43, pp. 379–404.

Klevmarken, N.A., Lupton, J., Stafford, F. (2003). Wealth Dynamics in the 1980s and 1990s: Sweden and the United States. *The Journal of Human Resources* 38 (2), pp. 322–353.

König, J., Schluter, C., Schröder, C. (2025). Routes to the Top. *Review of Income and Wealth* 71 (2), e70015.

Kuhn, M., Schularick, M., Steins, U. (2020). Income and Wealth Inequality in America, 1949–2016. *Journal of Political Economy* 128 (9), pp. 3469–3519.

Lee, H., Myers, D., Painter, G., Thunell, J., Zissimopoulos, J. (2020). The Role of Parental Financial Assistance in the Transition to Homeownership by Young Adults. *Journal of Housing Economics* 47, 101597.

Lersch, P., Longmuir, M., Schnitzlein, D. (2024). Intergenerational Persistence of Wealth. *Research Handbook on Intergenerational Inequality*, pp. 86–99. Edward Elgar Publishing.

Levell, P., Sturrock, D. (2023). Using Understanding Society to Study Intergenerational Wealth Mobility in the UK. *Fiscal Studies* 44, pp. 417–432.

Lindquist, M., Sol, J., Van Praag, M. (2015). Why Do Entrepreneurial Parents Have Entrepreneurial Children? *Journal of Labor Economics* 33 (2), pp. 269–296.

Mahler, L., Yum, M. (2024). Lifestyle Behaviors and Wealth-Health Gaps in Germany. *Econometrica* 92 (5), pp. 1697–1733.

Menchik, P. (1979). Inter-generational Transmission of Inequality: An Empirical Study of Wealth Mobility. *Economica* 46 (184), pp. 349–362.

Mogstad, M., Torsvik, G. (2023). Family Background, Neighborhoods, and Intergenerational Mobility. *Handbook of the Economics of the Family* 1 (1), pp. 327–387.

Mulligan, C. (1997). *Parental Priorities and Economic Inequality*. The University of Chicago Press.

Pfeffer, F. (2018). Growing Wealth Gaps in Education. *Demography* 55, pp. 1033–1068.

Pfeffer, F., Schoeni, R., Kennickell, A., Andreski, P. (2016). Measuring Wealth and Wealth Inequality: Comparing Two U.S. Surveys. *Journal of Economic and Social Measurement* 41, pp. 103–120.

Pfeffer, F., Killewald, A. (2018). Generations of Advantage. Multigenerational Correlations in Family Wealth. *Social Forces* 96 (4), pp. 1411–1442.

Sabelhaus, J. (2024). Intergenerational Wealth Persistence in the United States. Working Paper, Brookings Institution.

Saez, E., Zucman, G. (2016). Wealth Inequality in the United States since 1913: Evidence from Capitalized Income Tax Data. *The Quarterly Journal of Economics* 131 (2), pp. 519–578.

Shiro, A., Pulliam, C., Sabelhaus, J., Smith, E. (2022). Stuck On The Ladder: Intragenerational Wealth Mobility in the United States. Working Paper, Brookings Institution.

Siminski, P., Yu, S.H. (2022). The Correlation of Wealth Between Parents and Children in Australia. *The Australian Economic Review* 55 (2), pp. 195–214.

Smith, M., Zidar, O., Zwick, E. (2023). Top Wealth in America: New Estimates Under Heterogeneous Returns. *The Quarterly Journal of Economics* 138 (1), pp. 515–573.

Staiger, M. (2023). The Intergenerational Transmission of Employers and the Earnings of Young Workers. Unpublished Manuscript, Opportunity Insights Harvard University.

Steckel, R. (1990). Poverty and Prosperity: A Longitudinal Study of Wealth Accumulation, 1850–1860. *The Review of Economics and Statistics* 72 (2), pp. 275–285.

Steckel, R., Krishnan, J. (2006). The Wealth Mobility of Men and Women during the 1960s and 1970s. *Review of Income and Wealth* 52 (2), pp. 189–212.

Straub, L. (2019). Consumption, Savings, and The Distribution of Permanent Income. Unpublished Manuscript, Harvard University.

Van Langenhove, C. (2025). Saving Rate Heterogeneity across the Wealth Distribution in the United States. Available at SSRN 5909823.

Van Langenhove, C. (2026). Intergenerational Transfers, Wealth Inequality and Wealth Mobility in the United States. Forthcoming.

Wagner, S., Boertien, D., Gørtz, M. (2020). The Wealth of Parents: Trends Over Time in Assortative Mating Based on Parental Wealth. *Demography* 57 (5), pp. 1809–1831.

A Data

A.1 Waves & samples

I use data from the Panel Study of Income Dynamics (PSID). The PSID ran annually from 1968 to 1997 and biennially from 1999 to 2021. All waves report gross main housing value, main housing mortgage debt, and rents paid. The 1984, 1989, 1994, and 1999–2021 waves add questions about other assets and debts. These questions allow defining household wealth.

The original 1968 PSID sample consists of two subsamples. First, the SRC subsample (Survey Research Center) is nationally representative. Second, the SEO sample (Survey of Economic Opportunities) oversamples low-income families. The PSID added a Latino subsample in 1990 but dropped it from 1995. In 1997 and 2017, the PSID added two representative immigrant subsamples. For each subsample, the PSID tracks original household members, their descendants, and individuals who joined through relationships.

Economic research using the PSID typically focuses on the SRC subsample (Cooper et al., 2019; Heathcote et al., 2010; Kaplan et al., 2014; Straub, 2019; Van Langenhove, 2025). I follow this approach. I also include the two immigrant samples as a robustness check. The Online Supplement confirms that conclusions hold with their inclusion.

I define two core samples. Let N denote the total number of households responding in at least one year between 1969 and 2021. A specific household carries subscript i:

$$\mathcal{T}_\Omega = \{1969, 1970, \ldots, 1997, 1999, 2001, \ldots, 2021\} \tag{3}$$

$$\Omega = \{\mathbf{I}_i^\Omega(t) \mid i = 1, 2, \ldots, N,\ t \in \mathcal{T}_\Omega\} \tag{4}$$

where $\mathcal{T}_\Omega$ collects the years for full sample Ω and $\mathbf{I}^\Omega$ denotes the available PSID variables. I exclude 1968 due to its high outlier count. The reduced sample is:

$$\mathcal{T}_\Psi = \{1984, 1989, 1994, 1999, 2001, \ldots, 2021\} \tag{5}$$

$$\Psi = \{\mathbf{I}_i^\Psi(t) \mid i = 1, 2, \ldots, N,\ t \in \mathcal{T}_\Psi\} \tag{6}$$

where $\mathcal{T}_\Psi$ collects the years for reduced sample Ψ and $\mathbf{I}_i^\Psi$ the available PSID variables. It holds that $\mathbf{I}^\Psi = [\mathbf{I}^\Omega, \mathbf{I}^\Phi]$, with $\mathbf{I}^\Phi$ the additional variables exclusive to Ψ.

A.2 Definitions

Unit of analysis The PSID unit of analysis is the family unit. Pfeffer et al. (2016) argue that family units need not coincide with households. For example, an adult child returning home remains a separate family unit. Yet this situation is typically temporary. I therefore equate family units to households.

Wealth & wealth ranks Full sample Ω contains gross main housing (h), main housing mortgages (m), and rental payments (r). Reduced sample Ψ adds business, equity, fixed-income, and pension holdings, plus gross other housing. On the liability side, Ψ adds other housing debt and non-mortgage debt. I define household wealth w as total assets minus total debts. The definition excludes Social Security wealth and defined-benefit pension wealth, neither of which is observed in the PSID. This exclusion is standard in the PSID wealth mobility literature (Pfeffer & Killewald, 2018; Fisher & Johnson, 2023). Because Social Security wealth is more equally distributed than financial wealth, including it would compress wealth rank differences and mechanically increase measured mobility. Appendix C describes the treatment of defined-contribution pension wealth, which is included from 1999. For household i at time t, I compute w only if all categories are reported. A missing category classifies the household as a non-respondent at t.

The ultimate object of interest is the wealth rank κ. Let N_t denote the number of responding households at t. I define wealth rank $\kappa_i(t)$ for household i at time t as:

$$\kappa_i(t) = \left\lceil \frac{100 \times \left(1 + \sum_{k=1}^{N_t} \mathbf{1}(w_k(t) < w_i(t))\right)}{N_t} \right\rceil \tag{7}$$

where $\mathbf{1}(\cdot)$ is an indicator function and $\lceil \cdot \rceil$ is the ceiling function. This formula places ranks into integer bins from 1 to 100. Since $w \in \mathbf{I}^{\Phi}$, the same applies to κ: $\kappa_i \in \mathbf{I}^{\Phi}$.

Outliers & non-response PSID wealth data face two challenges. First, non-response is substantial. Bracketing partially mitigates this problem. I apply it whenever available (Appendix C). Second, asset and debt variables in Ψ lack harmonization over time. Both Ψ and Ω contain measurement errors. I align wealth categories across periods (Appendix C). I also apply variable-specific outlier corrections (Appendix C) and general outlier corrections (Online Supplement).

A.3 PSID-validation

I validate the PSID against the top-wealth-adjusted Survey of Consumer Finances (SCF). Figure 12 compares aggregate wealth trajectories. Figure 13 compares wealth shares.

The PSID systematically underestimates all wealth categories relative to the SCF (Figure 12). Pfeffer et al. (2016) and Insolera et al. (2021) document this finding. The gap is largest for net business holdings. The PSID accurately captures the time evolution of wealth and its components.

Wealth shares in the PSID track those in the SCF closely (Figure 13). Both datasets show a slight increase in inequality since the early 1980s. The PSID underestimates top wealth inequality (Pfeffer et al., 2016; Cooper et al., 2019). In 2019, the top 10% wealth share (including pensions) equals 62% in the PSID versus 77% in the SCF. The Online Supplement confirms this top-wealth bias using household counts.

Figure 12: Average wealth levels per household (for total wealth and its underlying categories).

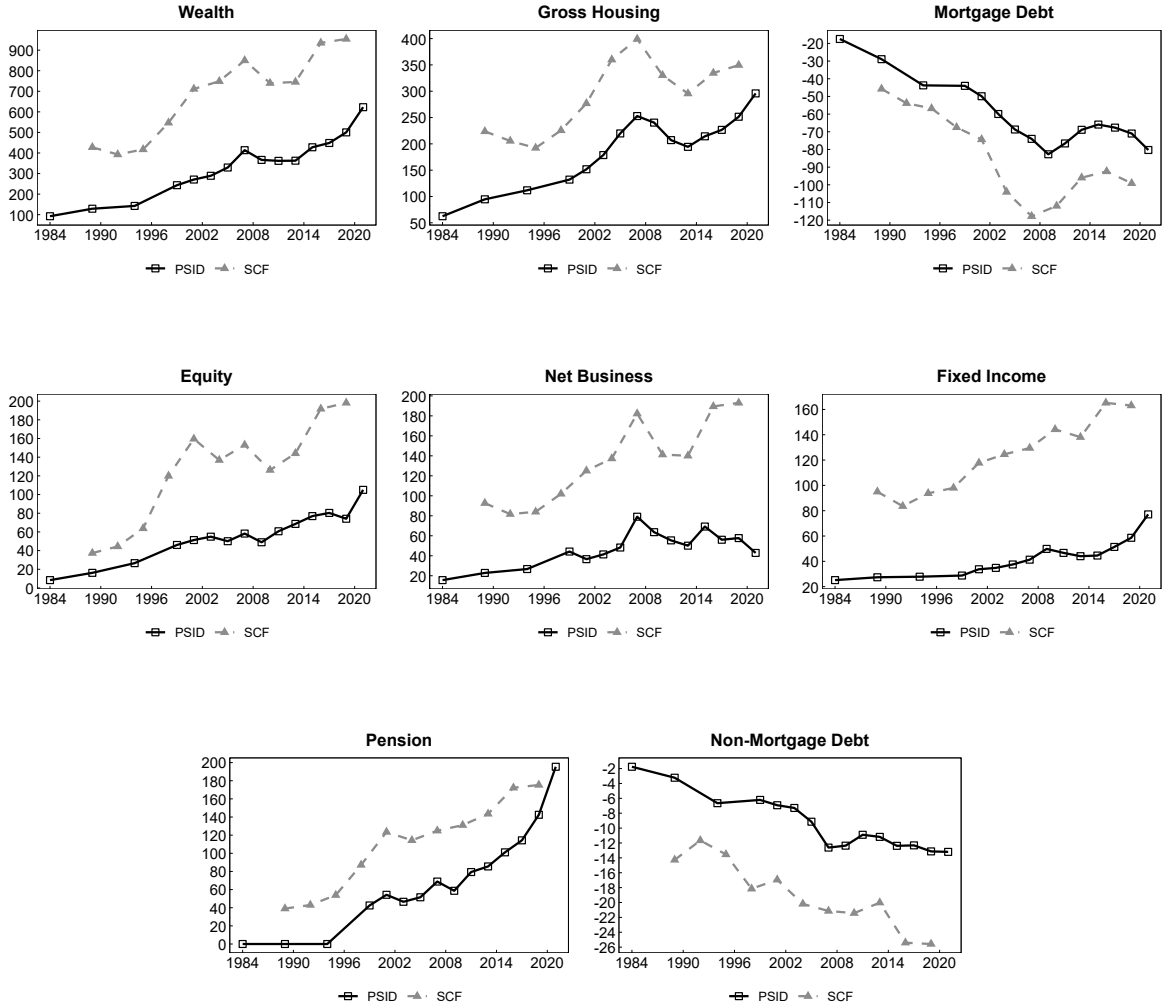

Note: Average household holdings (thousands of nominal dollars) per wealth component. Solid lines show PSID, dashed lines show top-wealth-adjusted SCF.

Figure 13: Wealth shares (in %) in the PSID and SCF databases.

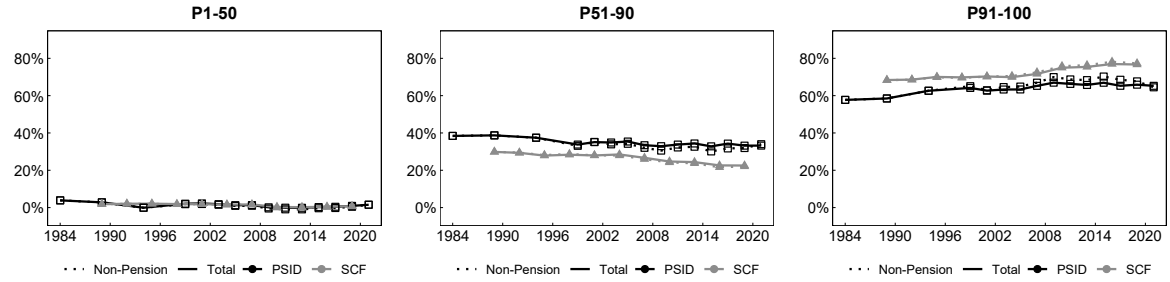

Note: Wealth shares by bracket (bottom 50%, middle 50–90%, top 10%). Colors distinguish non-pension and total wealth. Solid lines show PSID, dashed lines show SCF.

The SCF oversamples at the top of the wealth distribution; the PSID does not. One could supplement the PSID with Forbes 400 data, as Saez & Zucman (2016) do for distributional national accounts. I do not, for two reasons. First, the Forbes 400 composition changes annually, and incorporating it into a mobility study requires assumptions about entries and exits. Second, wealth mobility measures depend on household counts across the distribution, not on total wealth held. Missing a small number of top households barely affects these counts, whereas it creates large downward bias for wealth inequality measures. Correcting for top wealth is therefore less critical for wealth mobility than for wealth inequality.

A.4 Measurement error

Survey-reported wealth contains measurement error. Two features of the empirical design limit its impact.

First, I use ranks rather than levels. Errors that do not change who is richer than whom leave ranks unaffected. Even random noise has a smaller effect on ranks than on levels, because the rank transformation compresses outlying errors. The worst case would be misreporting that flips the ordering of households. PSID validation shows that underreporting concentrates at the very top (Section A.3), affecting wealth shares more than rank orderings.

Second, I summarize each individual's ranks as medians across two to five survey waves per lifecycle stage (Appendix E). The median filters out single-wave reporting errors. Any remain-

ing error in the regressor attenuates β toward zero. Estimated persistence is therefore a lower bound on true persistence.

B Summary statistics

B.1 Sample restrictions

All analyses share four restrictions. First, the sample is limited to SRC households. Second, I allocate household wealth to individuals based on household status (Section 3.3). Third, I rank individuals within ten-year birth cohorts at each survey wave on a scale from 1 to 100. Fourth, I summarize each individual's ranks as medians within five-year lifecycle stages (ages 30–34, 35–39, . . . , 70–74).

The analyses differ in sample composition and minimum observation thresholds:

- *Two-generational (parent–child).* The unit of observation is a child–parent pair observed at the same lifecycle stage. The pooled sample requires at least 1,500 pairs per stage combination. Cohort-level analyses require at least 500 pairs.
- *Three-generational (grandparent–grandchild).* The unit of observation is a grandchild–grandparent pair. Grandchildren are observed at ages 30–39 and grandparents at ages 40 and above. The pooled sample requires at least 1,500 pairs per stage combination. Cohort-level analyses require at least 500 pairs.
- *Intra-generational, working life (ages 30–54).* Balanced panel: individuals must be observed at both ages 30–34 and 50–54. Birth cohorts with fewer than 250 individuals are excluded.
- *Intra-generational, older age (ages 55–74).* Balanced panel: individuals must be observed at both ages 55–59 and 70–74. Birth cohorts with fewer than 250 individuals are excluded.
- *Within-family interdependence.* The sample consists of individuals in the intra-generational working life sample for whom at least one parent is also observed during the same calendar period.

All analyses report results for two wealth rank series: actual wealth ranks κ^{Ψ} (1984 onwards) and ML-proxied wealth ranks $\hat{\kappa}^{\Omega}$ (1969 onwards). The proxy sample is larger because it covers additional years.

B.2 Sample sizes

Tables 2 to 6 report sample sizes for each analysis.

Table 2: Sample sizes: two-generational (parent–child) analysis.

Lifecycle stage	N (actual)	N (proxy)
30–34	3,132	5,362
35–39	2,067	3,910
40–44	2,525	4,716
45–49	—	3,764
50–54	—	3,034
55–59	—	2,219
60–64	—	1,618

Note: N is the number of unique child–parent pairs where both generations are observed at the same lifecycle stage (e.g., both at ages 30–34). N (actual) counts pairs with direct wealth data (1984 onwards, κ^{Ψ}). N (proxy) counts pairs with ML-proxied wealth ranks (1969 onwards, $\hat{\kappa}^{\Omega}$). A dash ("—") indicates that the stage combination falls below the minimum sample size of 1,500 pairs. The sample is restricted to SRC-origin households.

Table 3: Sample sizes: three-generational (grandparent–grandchild) analysis.

Grandchild	Grandparent	N (actual)	N (proxy)
30–34	40–44	—	2,282
30–34	45–49	—	3,033
30–34	50–54	—	3,281
30–34	55–59	1,826	3,141
30–34	60–64	1,734	3,288
30–34	65–69	2,630	3,035
30–34	70–74	—	2,620
35–39	45–49	—	1,901
35–39	50–54	—	2,107
35–39	55–59	—	2,031
35–39	60–64	—	2,170
35–39	65–69	1,686	2,009
35–39	70–74	—	1,740

Note: N is the number of unique grandchild–grandparent pairs at each lifecycle stage combination. Rows show all combinations where grandchildren are observed at ages 30–39 and grandparents at ages 40 and above. N (actual) counts pairs with direct wealth data (1984 onwards, κ^{Ψ}). N (proxy) counts pairs with ML-proxied wealth ranks (1969 onwards, $\hat{\kappa}^{\Omega}$). A dash ("—") indicates that the stage combination falls below the minimum sample size of 1,500 pairs. The sample is restricted to SRC-origin households.

Table 4: Sample sizes: intra-generational analysis, working life (ages 30–54).

Birth cohort	*N*
Pooled	2,522
1946–1955	908
1956–1965	1,194
1966–1975	420

Note: *N* is the number of individuals observed at both the first and last lifecycle stage during working life (ages 30–54) (balanced panel). The sample is restricted to SRC-origin households with direct wealth data (1984 onwards, κ^{Ψ}). Individuals are ranked within their ten-year birth cohort. Birth cohorts with fewer than 250 individuals are excluded.

Table 5: Sample sizes: intra-generational analysis, older age (ages 55–74).

Birth cohort	*N*
Pooled	1,450
1926–1935	499
1936–1945	490
1946–1955	461

Note: *N* is the number of individuals observed at both the first and last lifecycle stage during older age (ages 55–74) (balanced panel). The sample is restricted to SRC-origin households with direct wealth data (1984 onwards, κ^{Ψ}). Individuals are ranked within their ten-year birth cohort. Birth cohorts with fewer than 250 individuals are excluded.

Table 6: Sample sizes: within-family interdependence analysis.

Birth cohort	N
Pooled	2,524
1946–1955	908
1956–1965	1,194
1966–1975	420

Note: N is the number of individuals in the intra-generational working life sample (ages 30–54, balanced panel) for whom at least one parent is also observed during the same calendar period. The sample is restricted to SRC-origin households with direct wealth data (1984 onwards, κ^{Ψ}). Individuals are ranked within their ten-year birth cohort.

B.3 Sample retention and attrition

The intra-generational analyses require balanced panels: individuals must be observed at both the first and last lifecycle stage of each phase. This requirement drops individuals who leave the sample.

Retention rates An individual is eligible if observed at the first lifecycle stage and born early enough to reach the last stage by 2021. I exclude birth cohorts with fewer than 250 balanced-panel individuals. Working life (ages 30–54) retains 2522 out of 4344 eligible individuals (58%). Older age (ages 55–74) retains 1450 out of 2349 (62%). Among those who drop out, most exhibit intermittent non-response rather than permanent attrition: 74% (working life) and 72% (older age) reappear at intermediate stages. Tables 7 and 8 report retention rates by initial wealth bracket.

Implications for persistence estimates Attrition is differential by wealth: bottom 50% individuals have lower retention (54% for working life, 56% for older age) than top 10% individuals (60% and 69%). The balanced panel underrepresents individuals who start poor and leave the sample, likely overstating wealth persistence. The estimated β is therefore an upper bound on true persistence. For older age, differential mortality reinforces this bias: individuals who die

Table 7: Retention rates by initial wealth bracket: working life (ages 30–54).

Initial bracket	N at first stage	N retained	Retention (%)
Bottom 50%	2,170	1,179	54
Middle 40%	1,738	1,081	62
Top 10%	436	262	60

Note: Initial bracket is based on the individual's within-cohort wealth rank at the first lifecycle stage (ages 30–34). Retention equals the fraction of individuals observed at both the first and last lifecycle stage (ages 30–34 and 50–54). The sample excludes individuals born after 1971, who could not have reached the last stage by the final PSID wave (2021). I use actual wealth ranks (κ^{Ψ}).

Table 8: Retention rates by initial wealth bracket: older age (ages 55–74).

Initial bracket	N at first stage	N retained	Retention (%)
Bottom 50%	1,174	662	56
Middle 40%	939	623	66
Top 10%	236	162	69

Note: Initial bracket is based on the individual's within-cohort wealth rank at the first lifecycle stage (ages 55–59). Retention equals the fraction of individuals observed at both the first and last lifecycle stage (ages 55–59 and 70–74). The sample excludes individuals born after 1951, who could not have reached the last stage by the final PSID wave (2021). I use actual wealth ranks (κ^{Ψ}).

before ages 70–74 may experience health-driven downward wealth mobility that the balanced panel does not capture (Section 5.3).

C Data definitions, outliers & non-response

C.1 Bracketing

Some households cannot report exact wealth values. For certain years and variables, the PSID offers bracketing questions that place the value in one of three intervals: $[0, x_1)$, $[x_1, x_2)$, or $[x_2, +\infty)$. I impute the midpoint for the first two brackets and $1.5 \times x_2$ for the open-ended bracket. I apply this procedure whenever available. The Online Supplement confirms that findings hold with and without bracketing.

C.2 Variable-specific definitions & outliers

C.2.1 Housing-related wealth categories

Main housing & rent The PSID does not report main housing mortgages in 1973–1975 and 1982. I interpolate them in three steps. First, I compute the mortgage ratio $\frac{h_i(t)}{m_i(t)}$ for all non-missing years in Ω. Second, I apply a distance-weighted interpolation (Online Supplement) over the missing years. Third, I recover $m_i(t)$ from the observed $h_i(t)$ and the interpolated ratio.

Rental payments are annual for 1969–1992 and monthly for 1993–2021. I annualize the latter period. Rents are missing for 1988–1989. I interpolate them using distance-weighted linear interpolation (Online Supplement). In 1970, a subset of homeowners report rents of 768. I set these outliers to zero.

Other housing The PSID reports other housing net of mortgage debt for 1984–2011 and gross for 2013–2021. Portfolio allocations (Appendix H.1) require gross values. I estimate a two-stage gradient-boosting model on SCF data (1989–2019) to predict the loan-to-value ratio on other housing. Stage 1 classifies whether a household carries other-housing mortgage debt. Stage 2 predicts the conditional loan-to-value ratio. I apply the trained model to PSID households for 1984–2011 to approximate gross other housing values and mortgages.

C.2.2 Non-housing wealth categories

Business & equity Business holdings are net of debts for 1984–2011. For 2013–2021, the PSID reports gross assets and debts separately. I compute the net measure. A handful of observations take unrealistically large negative values in a single wave. I set these outliers to zero.

Equity holdings equal the cumulative value of stocks in publicly traded corporations, stock mutual funds, and investment trusts. For 1984–1997, this variable also includes Individual Retirement Account (IRA) stock holdings. A few observations take unrealistically large negative values in a single wave. I correct these to zero.

Fixed income For 1984–1997, fixed income sums two survey questions. The first ("baseline fixed income") covers checking accounts, saving accounts, money market funds, certificates of deposit, government bonds, and Treasury bills, including IRAs. The second ("other") covers remaining assets, including bond funds and cash value of life insurance. For 1999–2017, the same questions apply, but the PSID asks IRA fixed income separately and excludes it. This change produces a minor trend break in 1999 (Figure 12). For 2019–2021, the baseline question splits into two parts. One covers checking, saving, and money market accounts. The other covers certificates, bonds, and bills. The "other" question remains unchanged. Fixed income then sums the three questions.

C.2.3 Pension wealth

Pension wealth equals defined contribution plans, IRAs, and private annuities. The PSID reports defined contribution values from 1999 onward. These values sum accounts held by the reference person and partner with the current and two previous employers. The PSID asks IRA and private annuity wealth separately from 1999 onward. Pension wealth therefore equals zero before 1999 (Figure 12). I set one-off outliers reaching negative billions to zero.

Two measurement issues arise. First, IRA wealth is embedded in equity and fixed income before 1999 and reported separately afterward. No reliable method separates it before 1999,

Figure 14: Ratio of pension to total wealth across the non-pension wealth distribution.

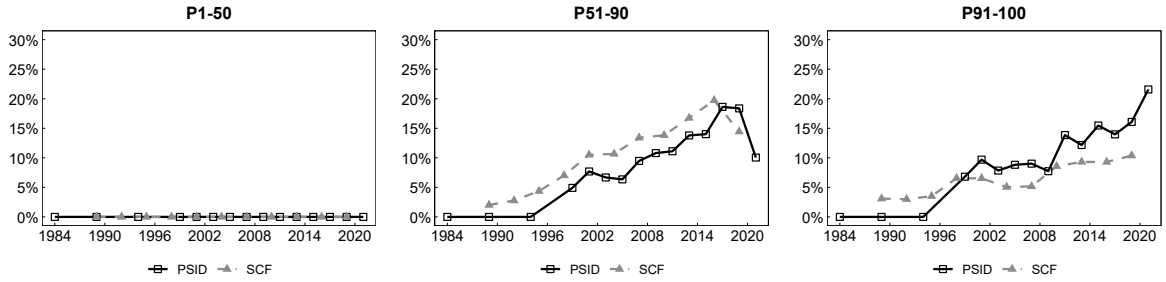

Note: Pension-to-total-wealth ratio by non-pension wealth bracket (bottom 50%, middle 50–90%, top 10%). PSID pensions equal zero before 1999 (not surveyed).

so I leave it in its original category for each period. This discrepancy affects portfolio shares but not total wealth or ranks. Second, defined contribution wealth enters w from 1999 but not before. The pension-to-total-wealth ratio is similar across wealth bins (Figure 14), suggesting this break does not differentially affect wealth ranks. The Online Supplement confirms that conclusions hold when restricting w to non-pension wealth.

C.2.4 Non-mortgage debt

The PSID reports non-mortgage debt as a single "other debt" variable for 1984–2009. In 2011, it splits this variable into four categories: credit card debt, student loans, medical debt, and debt to relatives. I sum all four. From 2013 onward, the PSID adds a fifth residual debt category, which I also include. The 2011 wave therefore understates non-mortgage debt slightly because it lacks the residual category. This gap is marginal: no trend shift appears in 2011 (Figure 12).

D ML proxies over the full sample Ω

D.1 Framework

The PSID records wealth only from 1984 (reduced sample $\mathcal{T}_\Psi$). This limits cross-cohort comparisons and three-generation analysis. Gross main housing value h and rental payments r are available over the full period $\mathcal{T}_\Omega$ (from 1969). I use these variables, together with other socio-economic characteristics, to predict wealth ranks before 1984.

The prediction model takes the form:

$$\hat{w}_i^\Omega(t) = \begin{cases} \hat{f}_h(\mathbf{x_h}) h_i^\Omega(t) & \text{if } h_i(t) > 0 \\ \hat{f}_r(\mathbf{x_r}) r_i^\Omega(t) & \text{if } h_i(t) = 0 \end{cases} \tag{8}$$

For homeowners ($h_i(t) > 0$), predicted wealth equals housing value times a scaling factor $\hat{f}_h$ that depends on household characteristics $\mathbf{x_h}$. For renters ($h_i(t) = 0$), predicted wealth equals rent times a scaling factor $\hat{f}_r$ that depends on $\mathbf{x_r}$. I observe housing values and rents directly. The scaling factors require estimation.

D.2 Common assumptions

Pfeffer & Killewald (2018) proxy wealth by housing values alone, setting $\hat{f}_h = C$ (a fixed constant) and $\hat{f}_r = 0$. Fisher & Johnson (2023) additionally use interest and dividend income, but their approach remains a simple imputation without optimization. In the simplest case:

$$\hat{w}_i^\Omega(t) = \begin{cases} C h_i^\Omega(t) & \text{if } h_i(t) > 0 \\ 0 & \text{if } h_i(t) = 0 \end{cases} \tag{9}$$

This proxy equates wealth to housing value for homeowners and zero for renters. For wealth mobility (where ranks matter, not levels), correctness requires three assumptions. First, housing values correlate positively with wealth. Second, this correlation is stable over time. Third, renters hold zero wealth.

A constant C is a strong simplification. Housing value and wealth correlate at 0.66, but the homeowner scaling factor (w/h) has a standard deviation of 2.23: two homeowners with identical housing values can have very different wealth levels. For renters, the median scaling factor equals zero, but a non-negligible share reports positive wealth (standard deviation 10.03). Accounting for household heterogeneity in scaling factors can therefore improve the proxy. I estimate two ML models (Section D.3) and compare them to four housing proxies (Section D.4). The ML models outperform all housing proxies (Section D.5).

D.3 ML-models

I construct a gradient-boosting (GB) model to predict $\hat{f}_h$ and $\hat{f}_r$. The Online Supplement develops an alternative multi-layer perceptron (MLP) model. I train and test both models on Ψ, estimating separately for homeowners and renters. Inputs $\mathbf{x_h}$ and $\mathbf{x_r}$ consist of household-level variables available over $\mathcal{T}_\Omega$. The models then predict over $\mathcal{T}_\Omega$. The Online Supplement contains the full GB derivation, the MLP model development, and diagnostic tests.

Input variables I select inputs $\mathbf{x_h}$ and $\mathbf{x_r}$ based on two criteria: the variable must be available over $\mathcal{T}_\Omega$ and must improve predictive performance. The selected inputs are:

1. Labor income $\frac{y_i(t)}{\bar{y}(t)}$: the household's labor income $y_i(t)$ normalized by the average labor income across all households $\bar{y}(t)$.

2. Capital income $\frac{\gamma_i(t)}{\bar{\gamma}(t)}$: the household's capital income $\gamma_i(t)$ relative to the average capital income across all households $\bar{\gamma}(t)$.

3. Household size $h_i^n \in [1, A]$: the number of individuals living in household i, comprising the reference person, partner, and children.

4. Household status $h_i^s \in \{0, 1, 2\}$: indicates whether the reference person is single (0), in a relationship with the partner (1), or married to the partner (2).

5. Age $h_i^a \in [1, B]$: the age of the oldest individual in the household (between the reference person or the partner).

6. Business ownership $n_i^b \in \{0, 1, 2\}$: indicates whether the household does not own a business (0), owns an unincorporated business (1), or owns an incorporated business (2).

7. Health status $h_i^h \in [0, 1]$: the proportion over the past four years in which at least one of the core household members was unable to work due to poor health.

8. Cars per adult $\frac{h_i^c}{\bar{h}(t)}$, with $h_i^c \in [1, C]$: the number of cars per adult owned by the household, normalized by the sample median at time t.

I apply outlier corrections to these inputs. Cars per adult is missing for 1973–1974 and 1987–1997. I interpolate using the distance-weighted procedure from the Online Supplement. The Online Supplement also lists the PSID questionnaire codes.

The homeowner inputs ($\mathbf{x_h}$) additionally include normalized housing values $h_i(t)/\bar{h}(t)$ and the mortgage ratio $m_i(t)/h_i(t)$. The renter inputs ($\mathbf{x_r}$) include normalized rents $r_i(t)/\bar{r}(t)$. These variables capture scale dependence between scaling factors and residence value. Wealthier households live in more expensive houses, but housing may decline as a share of total wealth.

Estimation & cross-validation I estimate the GB model over $\mathcal{T}_\Psi$, splitting observations into training and testing sets. The loss function is mean squared error (MSE). The GB model predicts scaling factors over $\mathcal{T}_\Omega$ as:

$$\hat{f}_h^{\text{GB}} = \hat{f}_h^{M_h^*}(\mathbf{x_h}) = \hat{f}_h^{(0)} + \sum_{m=1}^{M_h^*} \lambda_h^* g_h^{(m)}(\mathbf{x_h}) \tag{10}$$

$$\hat{f}_r^{\text{GB}} = \hat{f}_r^{M_r^*}(\mathbf{x_r}) = \hat{f}_r^{(0)} + \sum_{m=1}^{M_r^*} \lambda_r^* g_r^{(m)}(\mathbf{x_r}) \tag{11}$$

where the Online Supplement provides a full derivation. $\hat{f}^{(0)}$ is the initial guess and $g^{(m)}$ the weak learner at iteration m. The hyperparameters are boosting rounds M^*, learning rate λ^*, and maximum tree depth d^*. Substituting $\hat{f}_h^{\text{GB}}$ and $\hat{f}_r^{\text{GB}}$ into Equation 8 yields $\hat{w}_i^{\Omega}(t; \mathcal{M}_{\text{GB}})$.

I optimize hyperparameters via k-fold cross-validation, separately for homeowners and renters. The average cross-validation losses are:

$$\mathcal{L}_{\text{CV}}(M_h, d_h, \lambda_h) = \frac{1}{k} \sum_{j=1}^{k} \mathcal{L}^{(j)}(M_h, d_h, \lambda_h) \tag{12}$$

$$\mathcal{L}_{\text{CV}}(M_r, d_r, \lambda_r) = \frac{1}{k} \sum_{j=1}^{k} \mathcal{L}^{(j)}(M_r, d_r, \lambda_r) \tag{13}$$

with $k = 10$. The optimal hyperparameters minimize the cross-validation loss:

$$(M_h^*, d_h^*, \lambda_h^*) = \arg\min \mathcal{L}_{\text{CV}}(M_h, d_h, \lambda_h) \tag{14}$$

$$(M_r^*, d_r^*, \lambda_r^*) = \arg\min \mathcal{L}_{\text{CV}}(M_r, d_r, \lambda_r) \tag{15}$$

For homeowners, the optimal hyperparameters are $M^* = 140$, $d^* = 9$, $\lambda^* = 0.045$. For renters, they are $M^* = 90$, $d^* = 6$, $\lambda^* = 0.06$. The Online Supplement reports SHAP value summaries for both models.

D.4 Housing measures

I define four housing proxies as benchmarks, following Pfeffer & Killewald (2018). These proxies use limited information and no optimization.

The first proxy $\hat{w}_i^{\Omega}(t; \mathcal{M}_{\text{NP1}})$ follows Equation 9. Homeowner wealth equals C times housing value. Renter wealth equals zero. For rankings, the value of C is irrelevant as long as $C > 0$. The remaining three proxies refine the renter wealth estimate.

The second proxy is:

$$\hat{w}_i^{\Omega}(t; \mathcal{M}_{\text{NP2}}) = \begin{cases} C h_i^{\Omega}(t) & \text{if } h_i(t) > 0 \\ C \frac{r_i^{\Omega}(t)}{v(t)} & \text{if } h_i(t) = 0 \end{cases} \tag{16}$$

where $v(t)$ is the rental yield from Jordà et al. (2019). This proxy assumes uniform rental yields and approximates renter residence value as the inverse rental yield. It then equates

renter wealth to that value. Since median renter wealth equals zero, the last assumption is strong. The third proxy addresses this problem:

$$\hat{w}_i^{\Omega}(t;\mathcal{M}_{\text{NP3}}) = \begin{cases} \bar{C}_h h_i^{\Omega}(t) & \text{if } h_i(t) > 0 \\ \bar{C}_r \frac{r_i^{\Omega}(t)}{v(t)} & \text{if } h_i(t) = 0 \end{cases} \tag{17}$$

where $\bar{C}_h$ is the average homeowner scaling factor and $\bar{C}_r$ the average renter scaling factor, both computed over $\mathcal{T}_{\Psi}$:

$$\bar{C}_h = \frac{1}{n}\sum_{i=1}^{n} \frac{w_i^{\Psi}(t)}{h_i^{\Psi}(t)} \qquad \text{if } h_i(t) > 0 \tag{18}$$

$$\bar{C}_r = \frac{1}{n}\sum_{i=1}^{n} \frac{w_i^{\Psi}(t)}{r_i^{\Psi}(t)} v(t) \qquad \text{if } h_i(t) = 0 \tag{19}$$

The fourth proxy replaces means with medians to reduce outlier influence:

$$\hat{w}_i^{\Omega}(t;\mathcal{M}_{\text{NP4}}) = \begin{cases} \tilde{C}_h h_i^{\Omega}(t) & \text{if } h_i(t) > 0 \\ \tilde{C}_r \frac{r_i^{\Omega}(t)}{v(t)} & \text{if } h_i(t) = 0 \end{cases} \tag{20}$$

where $\tilde{C}_h$ and $\tilde{C}_r$ are the median analogues of Equations 18 and 19.

D.5 Performance comparison

From the wealth predictions of the ML models and housing proxies, I compute approximated wealth ranks:

$$\hat{\kappa}_i^{\Omega}(t;\chi) = \left\lceil \frac{100 \times \left(1 + \sum_{k=1}^{N_t} \mathbf{1}(\hat{w}_k^{\Omega}(t;\chi) < \hat{w}_i^{\Omega}(t;\chi))\right)}{N_t} \right\rceil \tag{21}$$

where $\chi = \{\mathcal{M}_{\text{GB}}, \mathcal{M}_{\text{MLP}}, \mathcal{M}_{\text{NP1}}, \mathcal{M}_{\text{NP2}}, \mathcal{M}_{\text{NP3}}, \mathcal{M}_{\text{NP4}}\}$.

I compare proxy wealth ranks ($\hat{\kappa}$) to actual ranks (κ) over the testing set using mean squared error (MSE), mean absolute error (MAE), and the share of predictions deviating by more than

Table 9: Model performance for housing and machine learning wealth proxies.

Across years

Proxy	MSE	MAE	≥ 25	≥ 50
NP1	474.28	16.01	0.21	0.04
NP2	896.93	23.41	0.41	0.10
NP3	451.22	15.87	0.21	0.03
NP4	554.16	18.01	0.28	0.04
MLP	259.61	11.69	0.11	0.01
GB	207.17	10.33	0.09	0.01

Across households

Proxy	MSE	MAE	≥ 25	≥ 50
NP1	446.26	15.16	0.39	0.09
NP2	894.28	22.97	0.59	0.20
NP3	420.02	14.97	0.37	0.08
NP4	521.29	17.08	0.45	0.10
MLP	246.95	11.10	0.25	0.03
GB	196.54	9.80	0.21	0.02

Note: Panel (a) averages metrics across years. Panel (b) averages metrics across household trajectories. MSE is in squared rank units, MAE in rank units. Percentage columns report misallocation shares (≥ 25 or ≥ 50 rank units). Lower is better. Testing set covers 30% of observations, stratified by year.

25 or 50 ranks. I compute each metric in two ways. Per year (averaged across years):

$$\mathcal{M}_t = \frac{1}{N_t} \sum_{i=1}^{N_t} m(a_{i,t}, p_{i,t}), \quad \mathcal{M} = \frac{1}{T} \sum_{t=1}^{T} \mathcal{M}_t \tag{22}$$

Per household (averaged across households):

$$\mathcal{M}_i = \frac{1}{T_i} \sum_{t \in \mathcal{V}_i} m(a_{i,t}, p_{i,t}), \quad \mathcal{M} = \frac{1}{I} \sum_{i=1}^{I} \mathcal{M}_i \tag{23}$$

where $\mathcal{V}_i$ is the set of valid time points for individual i and $m(a, p)$ is $(a - p)^2$ for MSE or $|a - p|$ for MAE.

The GB model outperforms all housing proxies and the MLP model (Table 9), reducing the root mean squared rank prediction error by 32% relative to the best housing proxy (NP3, average scaling factors). I therefore use GB predictions throughout. For simplicity:

$$\hat{w}_i(t) = \hat{w}_i^{\Omega}(t; \mathcal{M}_{\text{GB}}), \quad \hat{\kappa}_i(t) = \hat{\kappa}_i^{\Omega}(t; \mathcal{M}_{\text{GB}}) \tag{24}$$

Prediction errors remain (Table 9). The GB model misallocates 9% of households by more than 25 ranks in the average year (1% by more than 50 ranks). Over the full lifecycle, 21% of households experience at least one misallocation exceeding 25 ranks (2% exceeding 50 ranks).

Figure 15: Proportion of misallocated households per wealth bin (according to actual wealth) for the GB proxy and the third housing proxy.

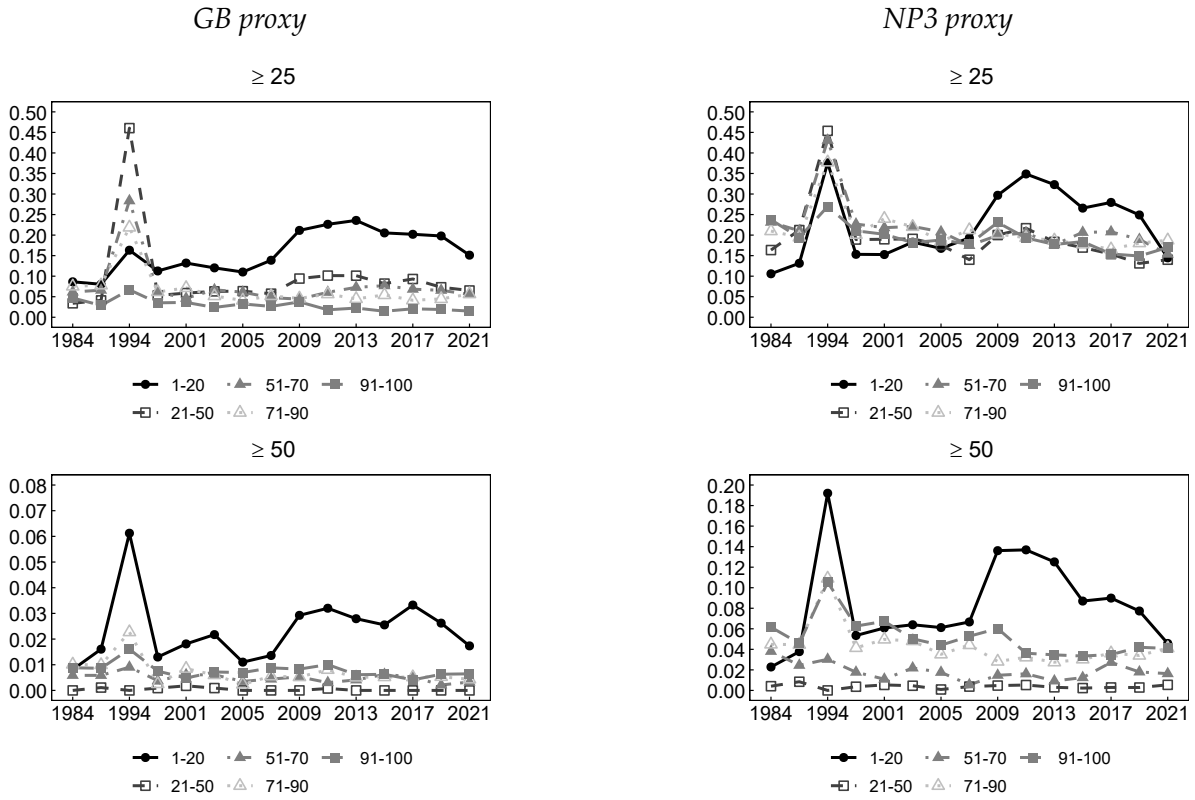

Note: Misallocation rates by actual wealth bin and survey year. Upper row shows the 25-rank threshold, lower row 50 ranks. Left panels show the GB proxy, right panels the best housing proxy (NP3). Wealth bins based on actual (not predicted) wealth.

Misallocations concentrate among poor households (bottom 20%), where wealth near zero makes small scaling-factor errors disproportionately consequential for ranks (Figure 15). Among poor households, misallocations spiked during the 2008 financial crisis. The GB proxy misallocates fewer households than the best housing proxy in all periods and across all wealth levels.

Proxy accuracy is stable across birth cohorts: neither the MAE nor the misallocation share varies systematically across cohorts (Online Supplement). The cross-cohort decline in wealth mobility documented in Sections 4 and 5 therefore reflects genuine changes in persistence, not deteriorating proxy performance for younger cohorts.

E Empirical strategy

E.1 Individual-level

Eligibility I track individual wealth mobility. Because individuals may switch households through marriage or divorce, I restrict the sample to individuals with control over household finances: reference persons and partners (legal spouses, cohabiting partners, and uncooperative legal spouses).

Wealth allocation I allocate household wealth w_i to individuals based on household status h_i^s. Singles ($h_i^s = 0$) receive all household wealth: $w_j = w_i$. Unmarried partners ($h_i^s = 1$) receive wealth in proportion to their labor income share (averaged over three waves): $w_j = \frac{y_j}{y_i} w_i$. Married couples ($h_i^s = 2$) split wealth equally: $w_j = \frac{1}{2} w_i$. I write $w_j(t)$ for the wealth of individual j at time t.

Wealth ranks I compute individual-level actual ranks $\kappa_j(t)$ and proxy ranks $\hat{\kappa}_j(t)$ following Equation 7:

$$\kappa_j(t) = \left\lceil \frac{100 \times \left(1 + \sum_{k=1}^{n_t} \mathbf{1}(w_k(t) < w_j(t))\right)}{n_t} \right\rceil \tag{25}$$

$$\hat{\kappa}_j(t) = \left\lceil \frac{100 \times \left(1 + \sum_{k=1}^{n_t} \mathbf{1}(\hat{w}_k(t) < \hat{w}_j(t))\right)}{n_t} \right\rceil \tag{26}$$

where n_t is the number of eligible individuals at time t, w is actual wealth, and $\hat{w}$ is GB-model predicted wealth (Appendix D).

E.2 Cohorts & lifecycle stages

Cohort assignment & lifecycle stages Each individual j has a birth year b_j. I assign individuals to ten-year birth cohorts $a_j = c(b_j)$, where $c(\cdot)$ maps birth years to cohort bins. The set of birth cohorts is Y, spanning $\{1866\text{–}75, \ldots, 2006\text{–}15\}$.

I define lifecycle stages as five-year age brackets: $\Xi = \{0\text{–}24, 25\text{–}29, 30\text{–}34, 35\text{–}39, 40\text{–}44, 45\text{–}49, 50\text{–}54, 55\text{–}59, 60\text{–}64, 65\text{–}69, 70\text{–}74, 75+\}$. At time t, individual j with age $t - b_j$ belongs to the stage $s \in \Xi$ that contains $t - b_j$. Time, cohort, and stage are therefore deterministically linked through the birth year.

Within-cohort wealth ranks Standard wealth ranks pool the entire population, so older individuals mechanically occupy higher positions. I instead rank individuals only against their birth cohort a:

$$\kappa_j(t;a) = \left\lceil \frac{100 \times \left(1 + \sum_{k=1}^{n_t^a} \mathbf{1}(w_k(t) < w_j(t))\right)}{n_t^a} \right\rceil \tag{27}$$

$$\hat{\kappa}_j(t;a) = \left\lceil \frac{100 \times \left(1 + \sum_{k=1}^{n_t^a} \mathbf{1}(\hat{w}_k(t) < \hat{w}_j(t))\right)}{n_t^a} \right\rceil \tag{28}$$

where n_t^a is the number of eligible individuals in cohort a at time t. The summation runs over individuals k in the same cohort a. These within-cohort ranks are the primary input for all wealth mobility analyses.

Median ranks within lifecycle stages I summarize ranks by taking the median across survey waves within each lifecycle stage s:

$$\kappa_j(s;a) = \text{Med}\left\{\kappa_j(t;a) \mid t \in \mathcal{T}_s(j)\right\} \tag{29}$$

where $\mathcal{T}_s(j) = \{t \in \mathcal{T} \mid (t - b_j) \in s\}$ collects the survey years when individual j's age falls in stage s. The proxy rank $\hat{\kappa}_j(s;a)$ follows the same definition. The resulting objects $\kappa_j(s;a)$ and $\hat{\kappa}_j(s;a)$ are the primary inputs for all wealth mobility analyses.

Taking the median serves four purposes: it smooths transitory measurement errors, reduces the impact of occasional non-response, attenuates noise from household transitions (marriage or divorce), and accommodates the non-uniform timing of PSID survey waves (annual through 1997, biennial afterward).

E.3 Proxy wealth & wealth ranks over Ψ

The preceding sections define actual wealth ranks $\kappa_j^{\Psi}(s;a)$ over $\mathcal{T}_{\Psi}$ and proxy ranks $\hat{\kappa}_j^{\Omega}(s;a)$ over $\mathcal{T}_{\Omega}$. I now define a third object: proxy ranks restricted to Ψ. This object isolates the effect of the proxy model from the effect of sample coverage:

$$\hat{w}_j^{\Psi}(s;a) = \hat{w}_j^{\Omega}(s;a)\Big|_{\mathcal{T}_{\Psi}}, \quad \hat{\kappa}_j^{\Psi}(s;a) = \hat{\kappa}_j^{\Omega}(s;a)\Big|_{\mathcal{T}_{\Psi}} \tag{30}$$

where $|_{\mathcal{T}_{\Psi}}$ indicates that the values are restricted to the time frame $\mathcal{T}_{\Psi}$.

Because $\hat{\kappa}_j^{\Psi}(s;a)$ covers the same period and individuals as $\kappa_j^{\Psi}(s;a)$, comparing the two reveals the proxy model's accuracy. Section 3.3 shows that outcomes based on $\hat{\kappa}_j^{\Psi}(s;a)$ align more closely with $\hat{\kappa}_j^{\Omega}(s;a)$ than with $\kappa_j^{\Psi}(s;a)$. Differences between actual and proxy results therefore reflect the proxy model, not sample coverage.

For reference, the relevant sets of wealth and rank variables are:

$$W = \{w_j^{\Psi}(s;a),\ \hat{w}_j^{\Omega}(s;a),\ \hat{w}_j^{\Psi}(s;a)\} \tag{31}$$

$$K = \{\kappa_j^{\Psi}(s;a),\ \hat{\kappa}_j^{\Omega}(s;a),\ \hat{\kappa}_j^{\Psi}(s;a)\} \tag{32}$$

E.4 Inter-generational linkages

The PSID enables family tree construction, linking individuals to parents and grandparents. I include biological and adoptive parents only. Each individual j has at most two parents $p(j) = \{p_1(j), p_2(j)\}$ and four grandparents:

$$g(p(j)) = \{g_1(p_1(j)), g_2(p_1(j)), g_1(p_2(j)), g_2(p_2(j))\} \tag{33}$$

For two-generational analyses, I compare parent and child ranks at identical lifecycle stages: $\kappa_j(s;a_j)$ versus $\kappa_{p(j)}(s;a_{p(j)})$. The stage s is the same, but the cohorts a_j and $a_{p(j)}$ differ. For three-generational analyses, I compare $\kappa_j(s;a_j)$ to $\kappa_{g(p(j))}(s';a_{g(p(j))})$. Comparing identical stages ($s =$

s') is infeasible because grandparental ranks are available only from age 40 onwards, while grandchild ranks are available only at ages 30–39.

E.5 Intra-generational lifecycle phases

For intra-generational analyses, I study wealth rank trajectories over two lifecycle phases: working life (ages 30–54, stages Ξ^{WL}) and older age (55–74, stages Ξ^{OA}). No individual in the PSID has data spanning both phases in full. Separating the two allows covering the full lifecycle using different birth cohorts.

F Inequality & wealth mobility metrics

I define five outcome measures: (i) wealth inequality and accumulation, (ii) rank-rank coefficients, (iii) transition probabilities, (iv) discretionary groups, and (v) hierarchical clustering. The intra-generational analyses use all five. The inter-generational analyses use (ii) through (iv).

Metrics (ii) through (v) compare two cross-sections of wealth ranks. Inter-generational analyses compare family members (parent-child or grandparent-grandchild) at identical or different lifecycle stages. Intra-generational analyses compare the same individual at an initial and final stage.

F.1 Wealth dynamics over the lifecycle

For each wealth bin b, I calculate wealth shares and median wealth-to-income ratios across lifecycle stages $s \in \Xi^{\text{WL}}$ or $s \in \Xi^{\text{OA}}$. Wealth shares are:

$$\lambda_b(s;a) = \frac{\sum_{j \in b} w}{\sum_j w} \tag{34}$$

where $w \in W$ is wealth. The median wealth-to-income ratio within bin b is:

$$\phi_b(s;a) = \text{Med}\left\{ \frac{w_j}{\bar{y}(t)} \mid j \in b \right\} \tag{35}$$

where $\bar{y}(t)$ is average labor income at time t. Depending on lifecycle phase, $a \in \text{Y}^{\text{WL}}$ or $a \in \text{Y}^{\text{OA}}$, and $s \in \Xi^{\text{WL}}$ or $s \in \Xi^{\text{OA}}$. I also compute the share of low-wealth and high-wealth individuals at each stage s. Low wealth is below $\bar{y}(s;a)$ and high wealth is above twenty times $\bar{y}(s;a)$:

$$\vartheta^l(s;a) = \frac{1}{|a|} \sum_{j \in a} \mathbf{1}\left(w_j < \bar{y}(s;a)\right), \quad \vartheta^h(s;a) = \frac{1}{|a|} \sum_{j \in a} \mathbf{1}\left(w_j > 20 \cdot \bar{y}(s;a)\right) \tag{36}$$

where $|a|$ denotes the number of individuals in birth cohort a, and $w \in W$.

F.2 Overall wealth mobility

Rank-rank coefficients I regress wealth ranks at a final stage ($s = f$) on ranks at the initial stage ($s = i$) using OLS:

$$\kappa_k(s = f) = \alpha + \beta\kappa_k(s = i) + \epsilon_k, \tag{37}$$

where α is the intercept, β captures wealth persistence, and ϵ_k is the error term for individual or family pair k.

F.3 Wealth mobility at the bottom and top

Transition matrices Transition matrices record the probability of moving from wealth bin b_{i} to b_{f} between stages $s = i$ and $s = f$. I assign individuals to bins based on $\kappa \in K$. The transition probability for cohort a is:

$$P(b_{\text{i}} \to b_{\text{f}})(a) = \frac{n_a(b_{\text{i}}, b_{\text{f}})}{\sum_{b_{\text{f}}} n_a(b_{\text{i}}, b_{\text{f}})} \tag{38}$$

where $n_a(b_{\text{i}}, b_{\text{f}})$ counts individuals in cohort a moving from b_{i} to b_{f}. The ex-ante and ex-post transition matrices for cohort a are:

$$T_{\text{EA}}(a) = [P(b_{\text{i}} \to b_{\text{f}})(a)]_{b_{\text{i}}, b_{\text{f}}}, \quad T_{\text{EP}}(a) = [P(b_{\text{i}} \to b_{\text{f}})(a)]_{b_{\text{f}}, b_{\text{i}}} \tag{39}$$

The two matrices use the same transition probabilities but condition on different margins. $T_{\text{EA}}(a)$ conditions on the starting bin: each column gives the probability of reaching each destination bin b_{f} given starting bin b_{i}. $T_{\text{EP}}(a)$ conditions on the ending bin: each column gives the probability of originating from each bin b_{i} given ending bin b_{f}.

Discretionary groups Using Equation 38, I calculate the relative occurrence of six discretionary groups. Three groups capture the bottom 20%. The steady poor (SP) start and end in the bottom 20%. The past poor (PP) move from the bottom 20% to the top 50%. The new poor (NP) fall from the top 50% to the bottom 20%. Three groups capture the top 10%. The steady

wealthy (SW) start and end in the top 10%. The past wealthy (PW) fall from the top 10% to the bottom 70%. The new wealthy (NW) rise from the bottom 70% to the top 10%.

Hierarchical clusters Transition matrices and discretionary groups require pre-specified thresholds and cover only a fraction of the sample. I complement them with hierarchical clustering, which groups individuals by the shape of their entire wealth rank trajectory without imposing bin cutoffs. I follow the four-step procedure of Audoly et al. (2024) (detailed in the Online Supplement). Because clustering requires full trajectories, I use it only for intra-generational analyses.

The procedure yields k clusters. I assign every individual to one cluster c. Each cluster is summarized by its average wealth rank trajectory $\bar{\kappa}_c(s)$, with $s \in \Xi^{\text{WL}}$ or $\in \Xi^{\text{OA}}$. Denoting $|C_c|$ as the cluster size:

$$\bar{\kappa}_c(s) = \frac{1}{|C_c|} \sum_{i \in C_c} \kappa_i(s) \tag{40}$$

I classify the k clusters into four groups based on their average trajectories $\bar{\kappa}_c(s)$. Let $\bar{\bar{\kappa}}_c = \frac{1}{|S|} \sum_s \bar{\kappa}_c(s)$ denote the grand mean across $|S|$ lifecycle stages. A cluster is *mobile* if the range of its average trajectory exceeds 20 rank points: $\max_s \bar{\kappa}_c(s) - \min_s \bar{\kappa}_c(s) > 20$. Among the remaining (stable) clusters, those with $\bar{\bar{\kappa}}_c \leq 40$ are classified as *bottom*, those with $\bar{\bar{\kappa}}_c \geq 80$ as *top*, and those with $40 < \bar{\bar{\kappa}}_c < 80$ as *middle*.

G Additional visualizations

This appendix reports additional figures for inter-generational and intra-generational wealth mobility, following the order of the main text.

Table 10: Share of families (in %) consolidating in the bottom 20% over two generations, across children's birth cohorts, for parents and children at identical lifecycle stages.

Variable	Stage	1946–1955	1956–1965	1966–1975	1976–1985	1986–1995	Pooled
$\hat{\kappa}^{\Omega}$	30-34	-	8.3	7.4	6.3	7.0	7.0
			(5.6, 11.0)	(6.3, 8.8)	(5.3, 7.3)	(5.6, 8.4)	(6.1, 7.7)
	35-39	-	6.2	6.7	7.5	-	7.1
			(4.2, 8.2)	(5.5, 8.2)	(5.9, 8.9)		(6.3, 7.7)
	40-44	10.5	7.5	7.6	8.6	-	8.2
		(8.2, 12.7)	(6.1, 8.9)	(6.4, 9.0)	(6.9, 10.3)		(7.3, 9.0)
	45-49	9.0	8.6	6.3	-	-	7.9
		(7.0, 11.0)	(7.1, 10.2)	(5.1, 7.6)			(7.1, 8.9)
	50-54	8.9	7.0	-	-	-	7.9
		(6.9, 11.2)	(5.9, 8.2)				(6.8, 8.9)
	55-59	10.5	8.4	-	-	-	9.2
		(7.9, 12.4)	(6.9, 9.6)				(7.9, 10.8)
	60-64	8.3	10.2	-	-	-	8.9
		(6.4, 10.6)	(8.4, 12.1)				(7.2, 10.7)

Note: Share of families where both parent and child rank in the bottom 20% at identical lifecycle stages. Proxy wealth $\hat{\kappa}^{\Omega}$. Parentheses show 95% bootstrapped confidence intervals (100 replications). Minimum 500 observations per cell. Appendix B reports sample sizes.

Table 11: Share of families (in %) consolidating in the top 10% over two generations, across children's birth cohorts, for parents and children at identical lifecycle stages.

Variable	Stage	1946–1955	1956–1965	1966–1975	1976–1985	1986–1995	Pooled
$\hat{\kappa}^{\Omega}$	30-34	-	2.3	3.4	2.7	3.2	3.0
			(0.7, 4.3)	(2.5, 4.5)	(1.9, 3.4)	(1.8, 4.8)	(2.4, 3.7)
	35-39	-	3.2	3.6	3.9	-	3.7
			(1.2, 5.3)	(2.8, 4.6)	(3.1, 4.7)		(3.0, 4.4)
	40-44	2.5	2.8	3.6	3.3	-	3.0
		(1.0, 4.7)	(1.9, 3.6)	(2.7, 4.3)	(1.9, 4.5)		(2.5, 3.6)
	45-49	2.6	3.2	3.7	-	-	3.2
		(1.6, 3.6)	(2.4, 4.0)	(2.6, 4.9)			(2.5, 3.8)
	50-54	2.0	2.6	-	-	-	2.6
		(1.4, 2.8)	(1.8, 3.4)				(1.8, 3.4)
	55-59	3.4	2.9	-	-	-	3.0
		(2.3, 4.7)	(1.8, 3.9)				(2.3, 3.8)
	60-64	2.9	3.3	-	-	-	3.1
		(2.0, 4.0)	(1.6, 5.0)				(2.3, 4.0)

Note: Share of families where both parent and child rank in the top 10% at identical lifecycle stages. Proxy wealth $\hat{\kappa}^{\Omega}$. Parentheses show 95% bootstrapped confidence intervals (100 replications). Minimum 500 observations per cell. Appendix B reports sample sizes.

Figure 17 reports ex-ante transition matrices for the two oldest lifecycle stages (50–54 and 55–59), complementing Figure 3 in the main text.

Figure 19 reports median wealth-to-income ratios across lifecycle stages by wealth bracket and birth cohort. During working life, all brackets accumulate wealth, with the top 10% growing faster in absolute terms than the bottom 50%. During older age, all brackets accumulate between ages 55 and 64 and decumulate thereafter.

Figure 16: Ex-post transition matrices $T_{\mathbf{EP}}(a)$ between parent and child wealth ranks at identical lifecycle stages for the pooled dataset.

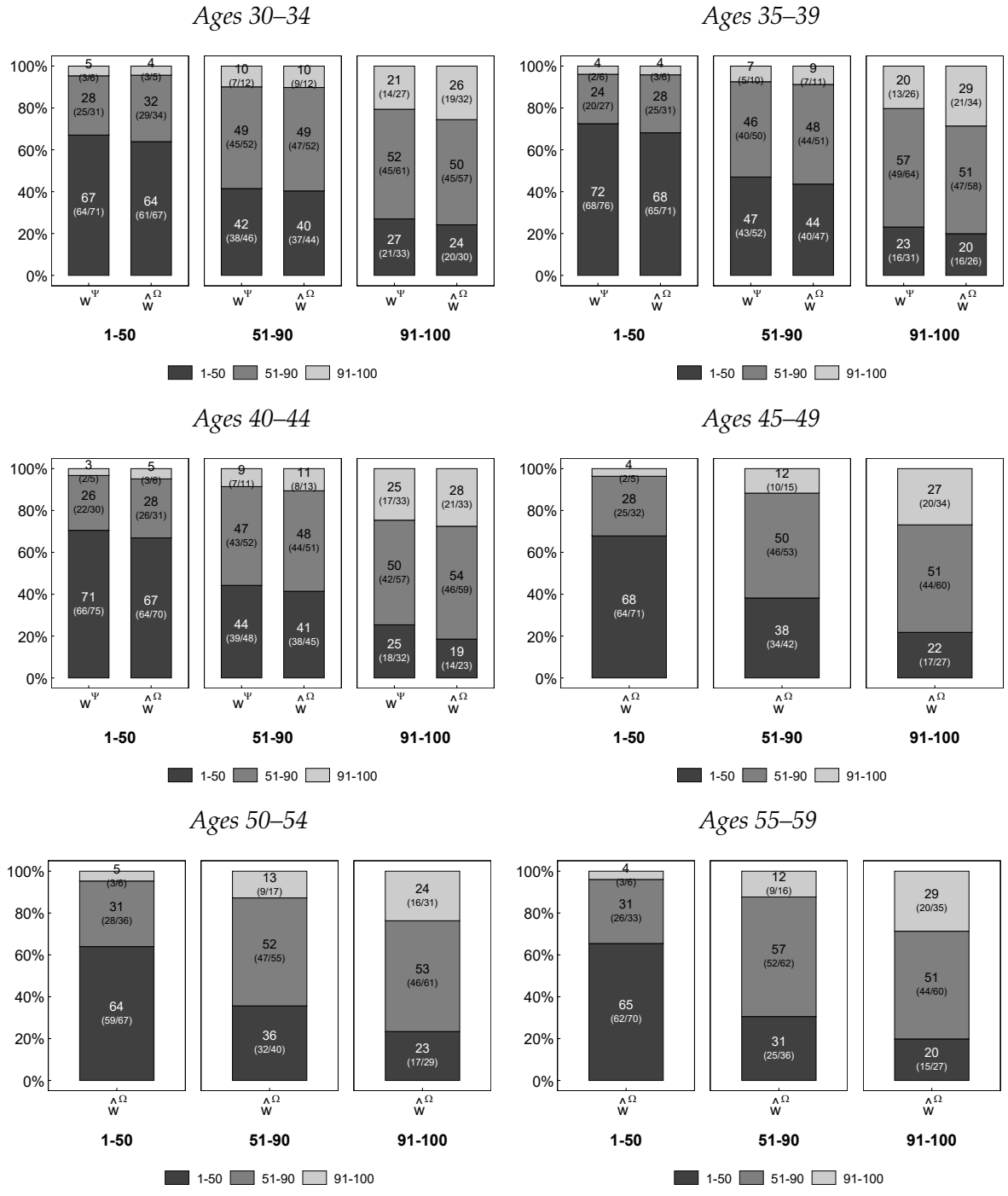

Note: Ex-post matrices condition on children's wealth brackets (bottom 50%, middle 50–90%, top 10%). Stacked bars show the probability of parental origin brackets. Columns within each panel distinguish actual wealth ranks (κ^{Ψ}) and proxy wealth ranks ($\hat{\kappa}^{\Omega}$). Numbers report transition probabilities (%). Parentheses show 95% bootstrapped confidence intervals (100 replications). Pooled dataset.

Figure 17: Ex-ante transition matrices $T_{\mathbf{EA}}(a)$ between parent and child wealth ranks at life-cycle stages 50–54 and 55–59 for the pooled dataset.

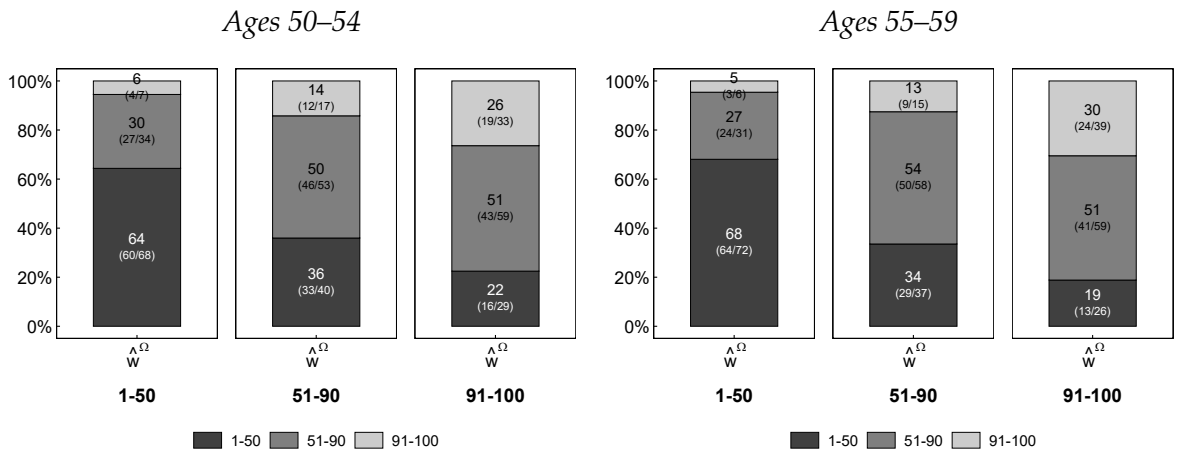

Note: Ex-ante matrices condition on parental wealth brackets (bottom 50%, middle 50–90%, top 10%). Columns within each panel distinguish actual wealth ranks (κ^{Ψ}) and proxy wealth ranks ($\hat{\kappa}^{\Omega}$). Numbers report transition probabilities (%). Parentheses show 95% bootstrapped confidence intervals (100 replications).

Figure 18: Transition probabilities for grandparents and grandchildren (solid lines) and parents and children (dotted lines) when (grand)children are aged 35–39.

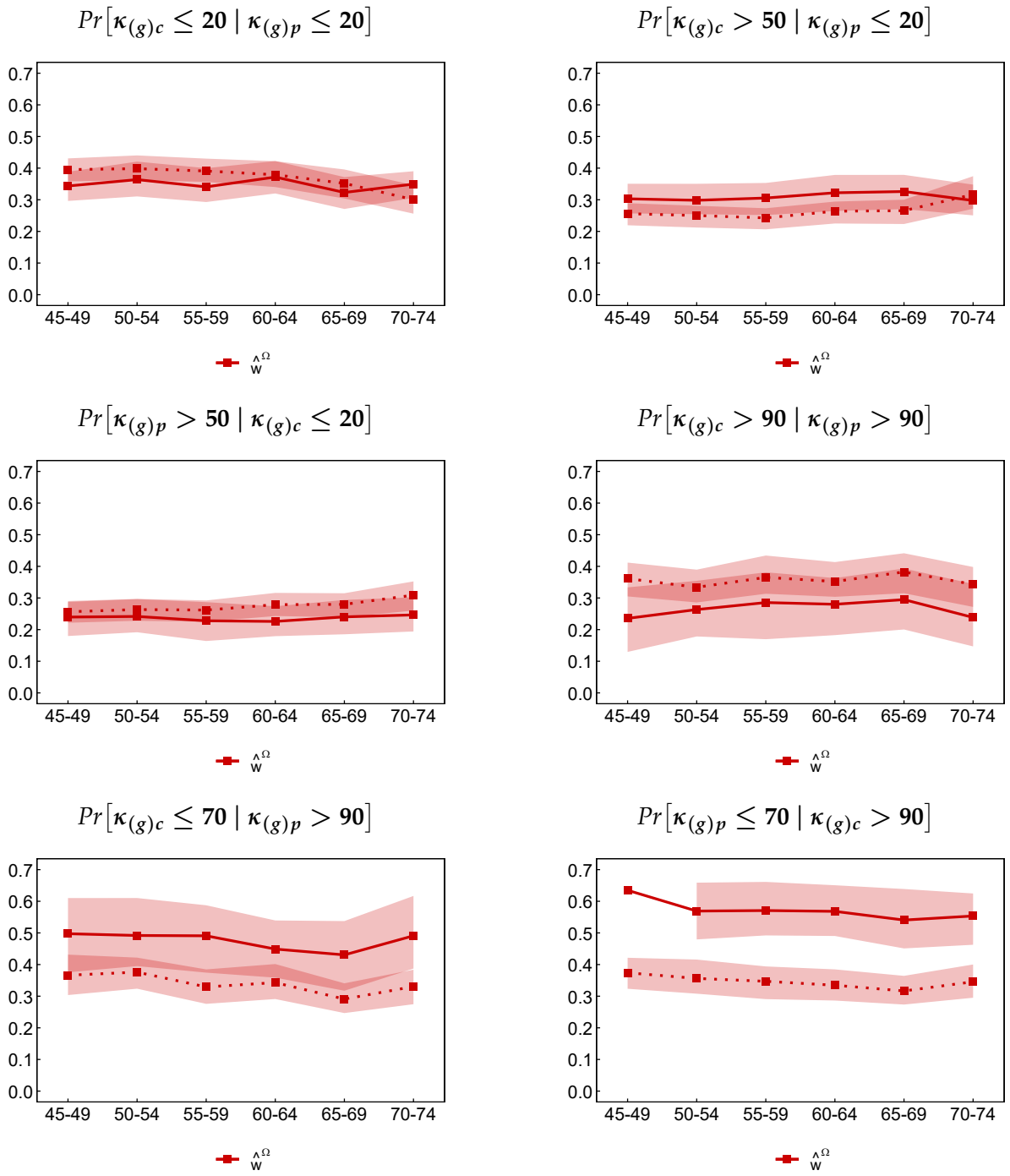

Note: (Grand)children fixed at ages 35–39. The horizontal axis varies (grand)parental stage. Solid lines show grandparent-grandchild, dotted lines parent-child. Subplot titles give conditional probabilities. Shaded ribbons show 95% bootstrapped confidence intervals (100 replications). Pooled dataset.

Figure 19: Wealth-to-income ratios ϕ_b across lifecycle stages by birth cohort, based on actual wealth levels w^{Ψ}.

Working life (ages 30–54)

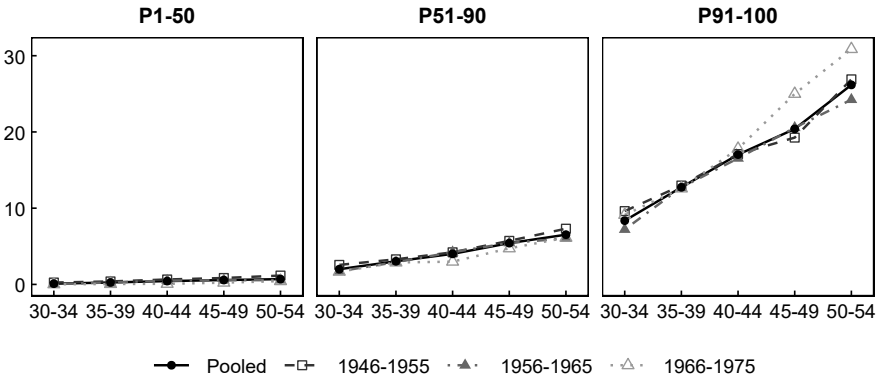

Older age (ages 55–74)

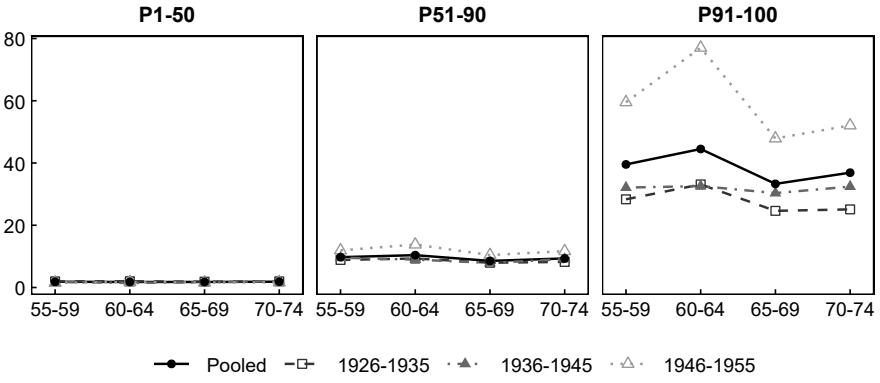

Note: Median wealth-to-income ratio (income = average annual labor income) by wealth bracket (P1–50, P51–90, P91–100) and birth cohort. Actual wealth w^{Ψ}. Working life and older age panels contain different individuals.

Figure 20: Proportion of high- and low-wealth individuals across birth cohorts, working life and older age, actual wealth levels w^{Ψ}.

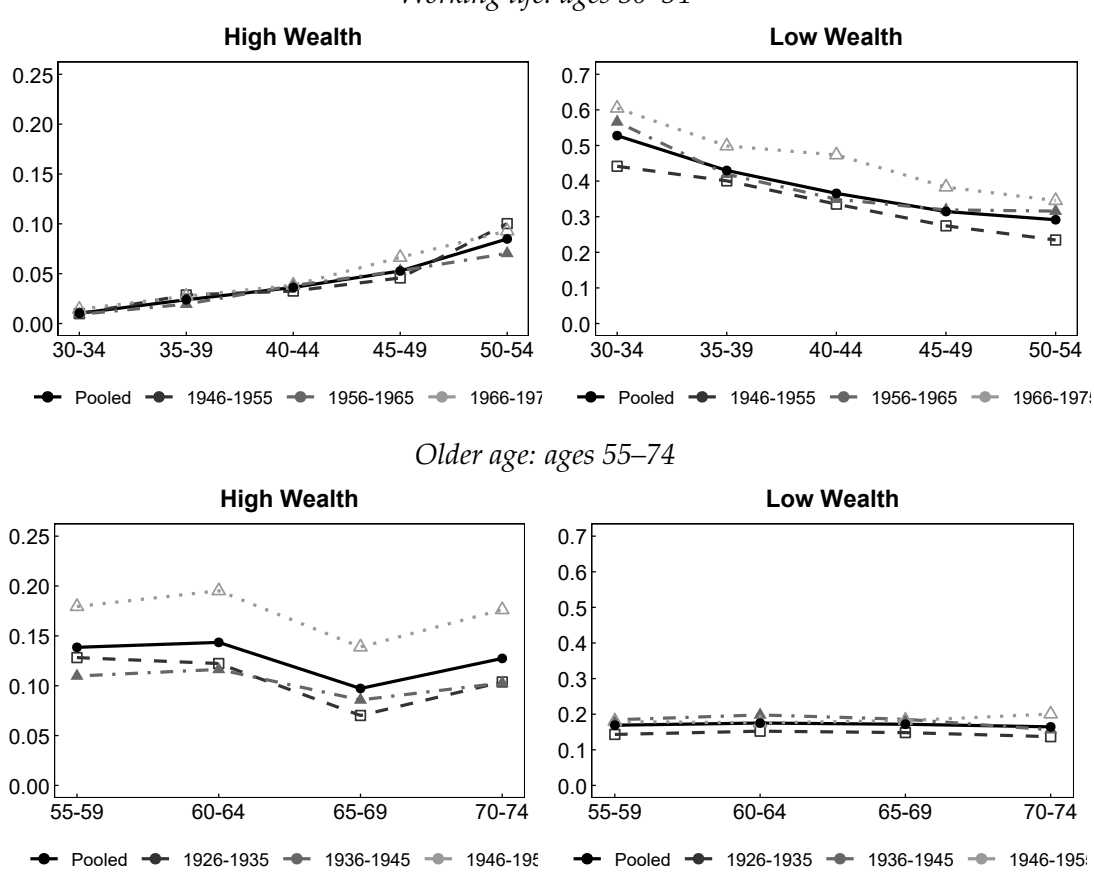

Note: High-wealth: wealth exceeds twenty times average labor income. Low-wealth: wealth below average labor income. Colors distinguish birth cohorts. Actual wealth w^{Ψ}. Working life and older age panels contain different individuals.

Figure 21: Ex-post transition matrices $T_{\mathbf{EP}}(a)$ during working life and older age for the pooled dataset.

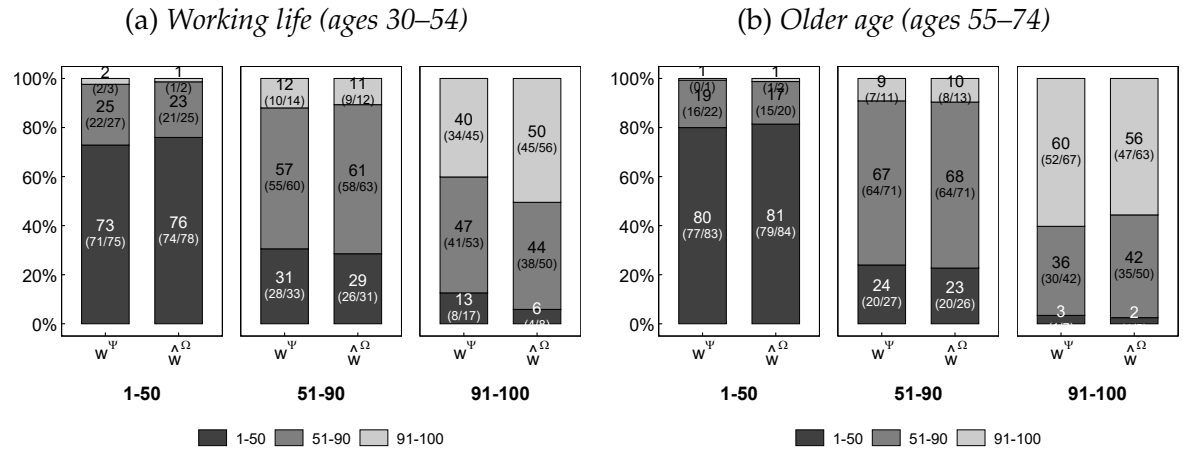

Note: Ex-post matrices condition on final wealth brackets (bottom 50%, middle 50–90%, top 10%). Left panel shows actual wealth ranks (κ^{Ψ}), ages 30–34 vs. 50–54. Right panel shows ages 55–59 vs. 70–74. Numbers report transition probabilities (%). Parentheses show 95% bootstrapped confidence intervals (100 replications).

Figure 22: Rolling two-stage transition probabilities for the wealthy discretionary groups, working life.

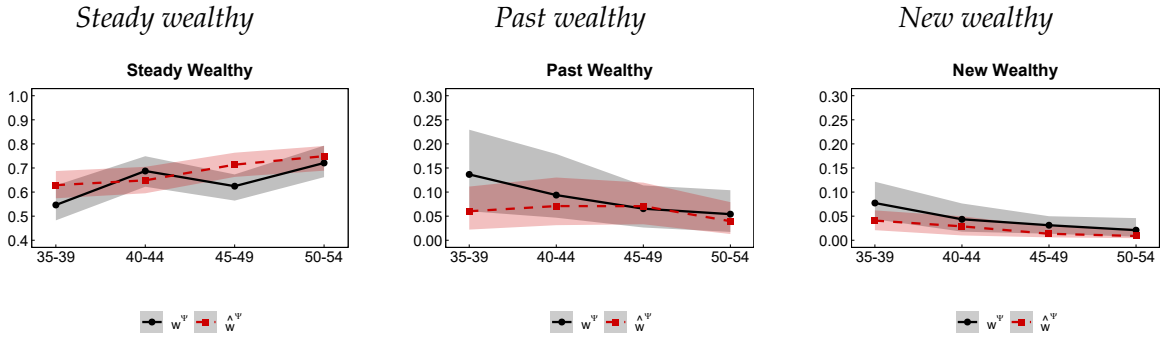

Note: Rolling two-stage transition probabilities between stages $k-1$ and k. Discretionary groups defined in Section 3.4. Colors distinguish actual (κ^{Ψ}) and proxy ($\hat{\kappa}^{\Omega}$) wealth ranks. Shaded ribbons show 95% bootstrapped confidence intervals (100 replications).

Figure 23: Rolling two-stage transition probabilities for the poor discretionary groups, working life.

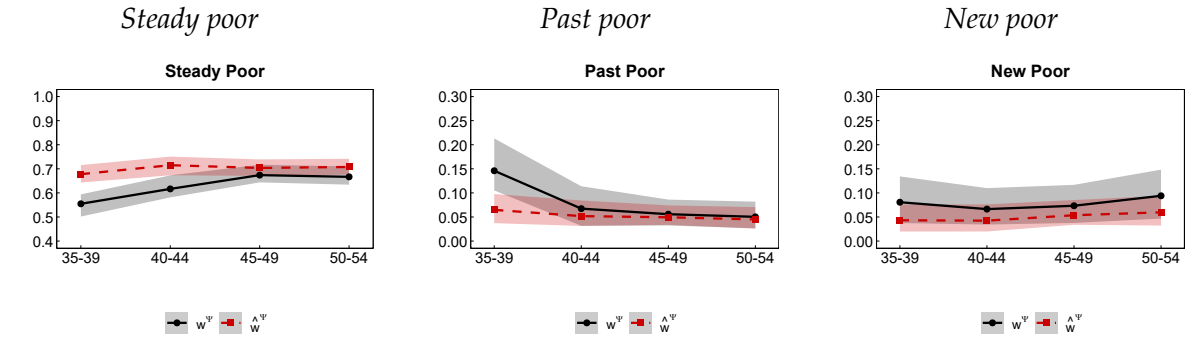

Note: Rolling two-stage transition probabilities between stages $k-1$ and k. Discretionary groups defined in Section 3.4. Colors distinguish actual (κ^{Ψ}) and proxy ($\hat{\kappa}^{\Omega}$) wealth ranks. Shaded ribbons show 95% bootstrapped confidence intervals (100 replications).

Figure 24: Rolling window analysis across birth cohorts, older age (ages 55–74).

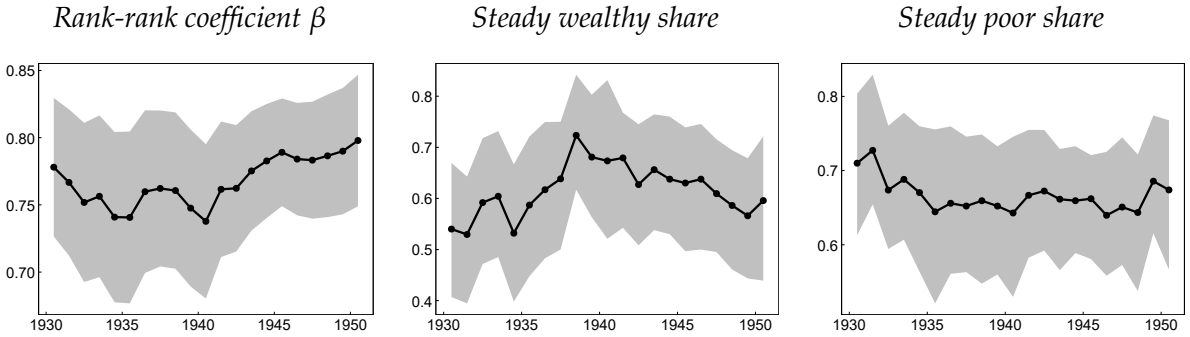

Note: Rolling ten-year birth cohort windows shifted by one year. Left panel shows the rank-rank coefficient β (ages 55–59 to 70–74). Middle and right panels show transition probabilities: the steady wealthy share (probability of starting and ending in the top 10%) and the steady poor share (probability of starting and ending in the bottom 20%). Actual wealth ranks (κ^{Ψ}). Shaded ribbons show 95% confidence intervals (HC1 for β, bootstrapped for shares with 100 replications). Minimum 300 individuals per window.

Figure 25: Rolling window analysis for remaining discretionary groups across birth cohorts, working life (ages 30–54).

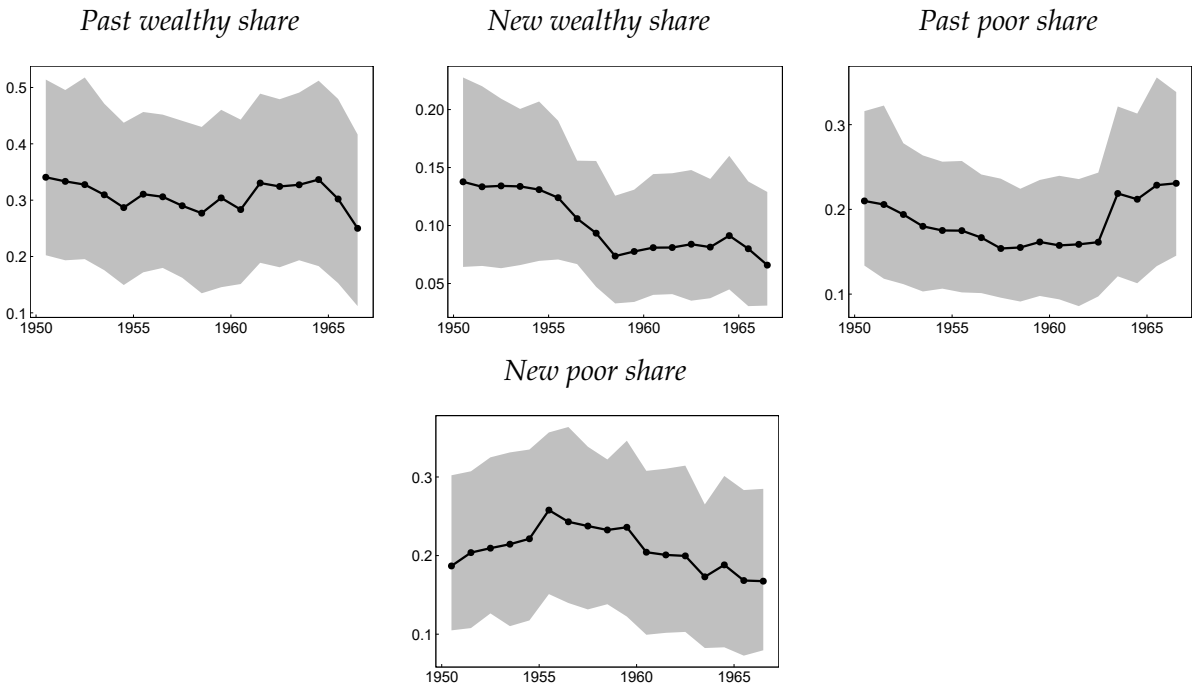

Note: Rolling ten-year birth cohort windows shifted by one year. Each panel shows a transition probability across cohort windows. Discretionary groups defined in Section 3.4. Actual wealth ranks (κ^{Ψ}). Shaded ribbons show 95% bootstrapped confidence intervals (100 replications). Minimum 300 individuals per window.

H Composition metrics and analysis

H.1 Metric definitions

I define the composition variables that characterize individuals within a sample, discretionary group, or cluster.

H.1.1 Labor income & non-mortgage indebtedness

I define the within-cohort labor income rank $\delta_j(t;a)$ by applying the ceiling function to labor income $y_j(t)$ within birth cohort a:

$$\delta_j(t;a) = \left\lceil \frac{100 \times \left(1 + \sum_{k=1}^{n_t^a} \mathbf{1}(y_k(t) < y_j(t))\right)}{n_t^a} \right\rceil \tag{41}$$

where n_t^a is the number of individuals in birth cohort a. I summarize $\delta_j(t;a)$ into lifecycle stages as $\delta_j(s;a)$ following Appendix E. I also calculate the non-mortgage debt-to-income ratio $\nu_j(t)$ (summarized over s as $\nu_j(s;a)$). This ratio equals non-mortgage debt divided by total household income. I aggregate both variables over a sample, group, or cluster g by taking the median.

H.1.2 Asset ownership & allocation

I define two types of measures. First, ownership dummies: a homeownership dummy $d_j^h(s;a)$ equals one if individual j belonged more often than not to a home-owning household during stage s. Business ownership dummies $d_j^{bu}(s;a)$ (unincorporated) and $d_j^{bi}(s;a)$ (incorporated) follow the same rule. I aggregate these dummies as the fraction of individuals with values equal to one. Second, conditional portfolio shares: equity $\alpha_j^e(s;a)$, housing $\alpha_j^h(s;a)$, and mortgage $\alpha_j^d(s;a)$, defined at the individual level as the household-level counterparts. I aggregate them by computing the median among owners.

H.1.3 Inter-vivos transfers & inheritances

The PSID contains two transfer-related variables. The first (available over Ω) records lump-sum payments (inheritances and insurance payouts) since the previous wave. I discard it: bracketed responses before 1982 and the inclusion of insurance payouts produce unreliable summary statistics. The second (available over Ψ) records gifts or inheritances since the previous wave. In 1984, the question retrospectively covers all prior transfers. The 1984–1989 waves allow two entries per household; from 1994, three. I apply bracketing where available and link household-level responses to individuals following Appendix E, defining received transfers at t as $l_j(t)$.

I compute cumulative transfers received up to each t and derive two metrics. First, a dummy $\iota_j^d(t)$ equals one if individual j received any transfer by t. I summarize it per stage s as $\iota_j^d(s;a)$ and aggregate as the fraction of recipients. Second, cumulative transfers relative to lifetime resources $\iota_j(t)$, following Black et al. (2025). Lifetime resources equal 35 times the average annual labor income, capitalized to the terminal year. I summarize $\iota_j(t)$ per stage as $\iota_j^s(s;a)$ and aggregate by taking the mean.

Three measurement issues affect $\iota_j^s(s;a)$. First, cumulative sums are sensitive to non-response. The 1984 question retrospectively covers all prior transfers; individuals who miss this wave have understated cumulative receipts. Random non-response across groups preserves relative differences. Second, household-to-individual allocation rules (Appendix E) may be imprecise for transfers tied to a specific household member. Third, self-reported transfers understate true values, especially at the top of the distribution.

H.1.4 Health & household composition

I define two measures. First, a health dummy $d_j^h(s;a)$ equals one if at least one core household member reports poor health during stage s. I aggregate it as the fraction of individuals in a poor-health household. Second, a household status variable $s_j^h(s;a)$ equals one if the individual is married or cohabiting. I aggregate it as the fraction of coupled individuals.

H.2 Results

Four findings emerge from Figure 26. First, non-mortgage debt participation and debt-to-income ratios are stable over working life but higher for recent cohorts. Second, homeownership rises with age, while the conditional housing portfolio share declines. The 1966–75 cohort has lower homeownership. Mortgage participation peaks at ages 40–44. Conditional mortgage-to-asset ratios fall over the lifecycle. Equity participation and conditional equity shares rise with age. Both were lower for the 1936–45 cohort. Business ownership rates are stable across ages and cohorts. Third, poor health and single-household status both increase with age. The 1966–75 cohort has a higher fraction of singles. Fourth, the fraction of transfer recipients and cumulative receipts rise strongly over working life. The 1936–45 cohort shows a lower fraction of recipients. This pattern reflects measurement error. This cohort received transfers before 1984, which the PSID captures imprecisely (Section H.1).

Figure 26: Socio-economic characteristics and inter-generational transfers of individuals in the working life sample.

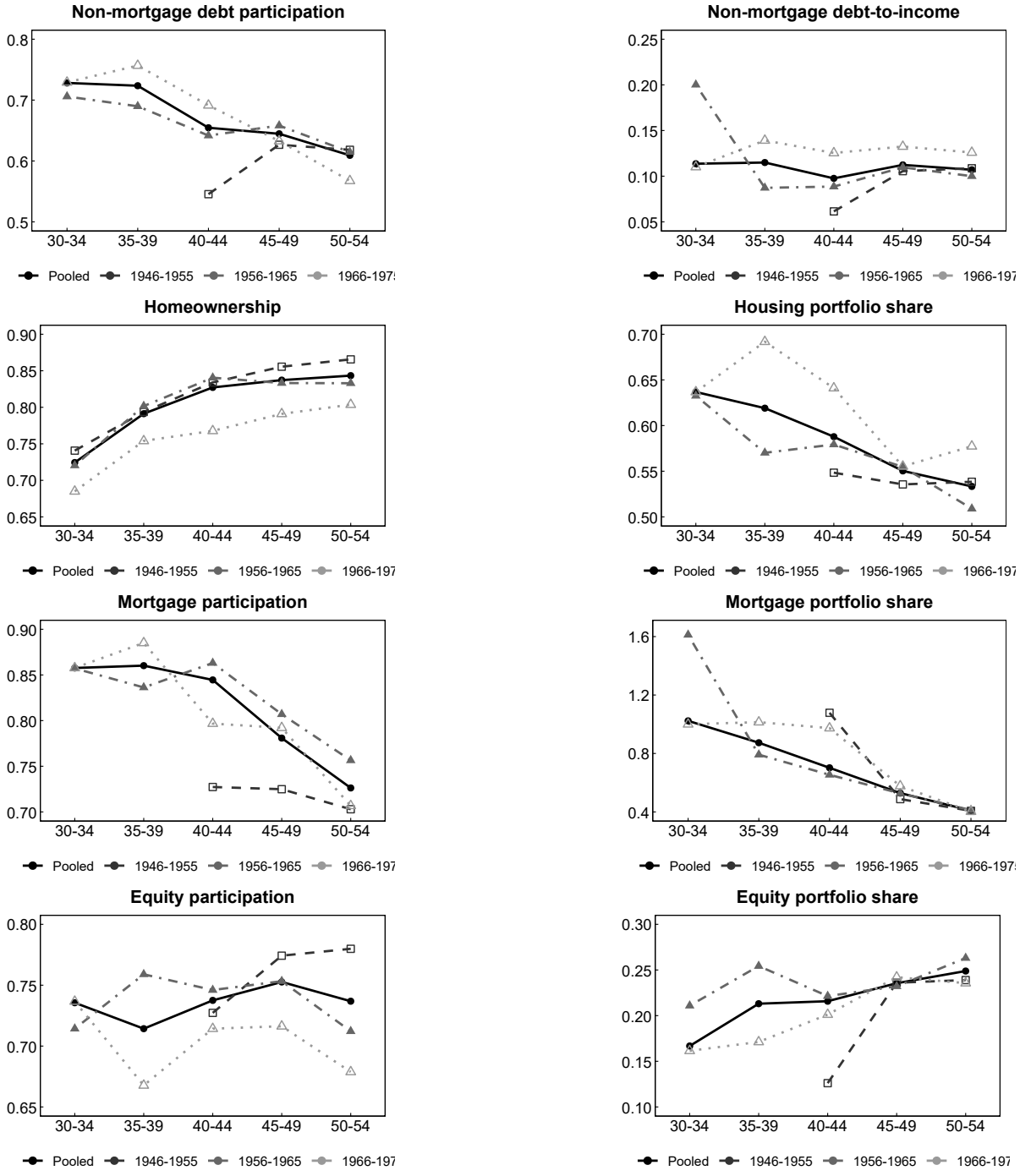

Note: Socio-economic characteristics by lifecycle stage and birth cohort, pooled working life sample. Left column shows proportions, right column conditional medians. Section H.1 defines all metrics.

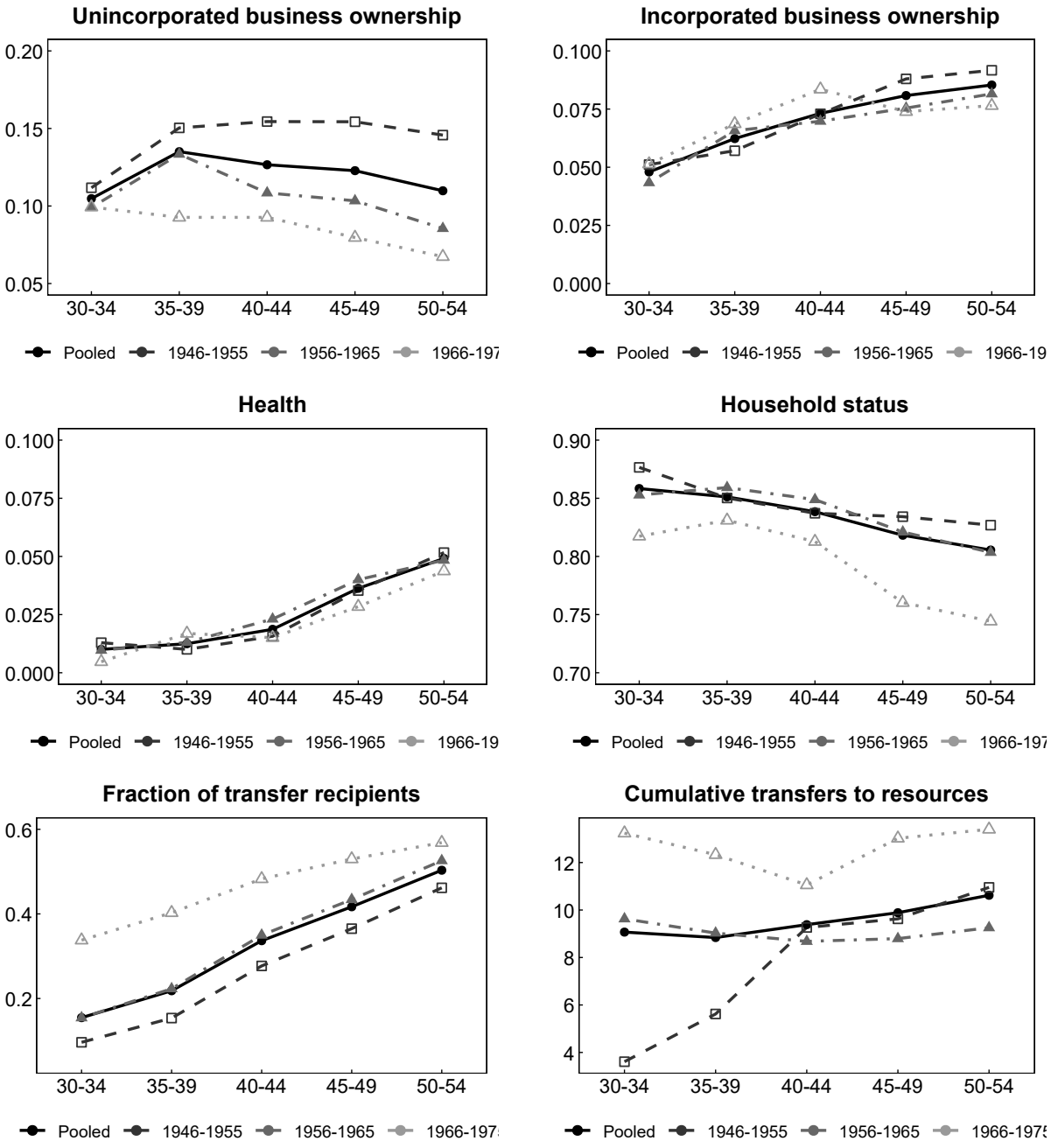

Note: Socio-economic characteristics by lifecycle stage and birth cohort, pooled working life sample. Left column shows proportions, right column conditional medians. Section H.1 defines all metrics.

Figure 27: Composition metrics per discretionary group across working lifecycle stages.

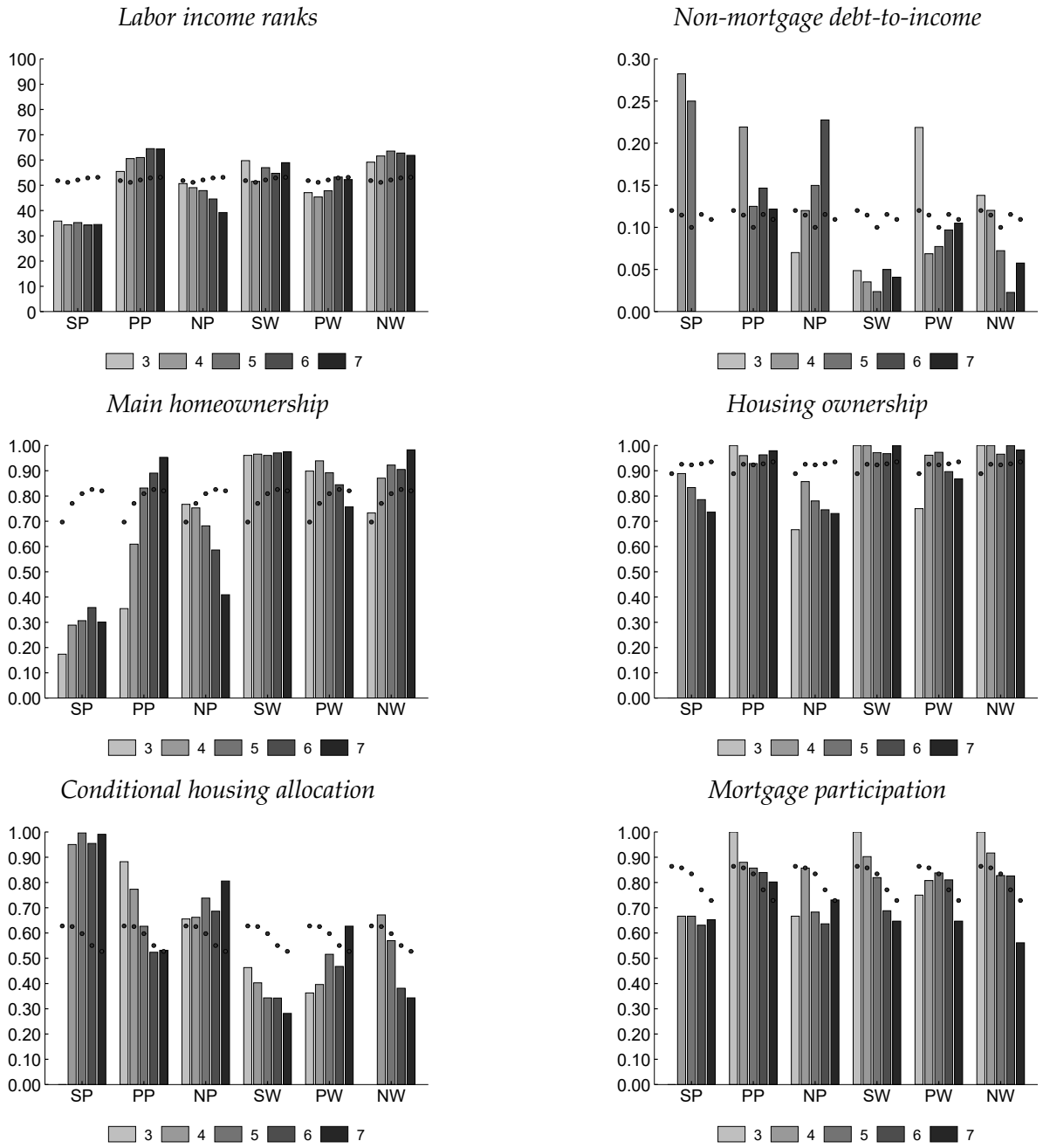

Note: Socio-economic characteristics by lifecycle stage for six discretionary groups (Section 3.4). Left column shows proportions, right column conditional medians. Section H.1 defines all metrics.

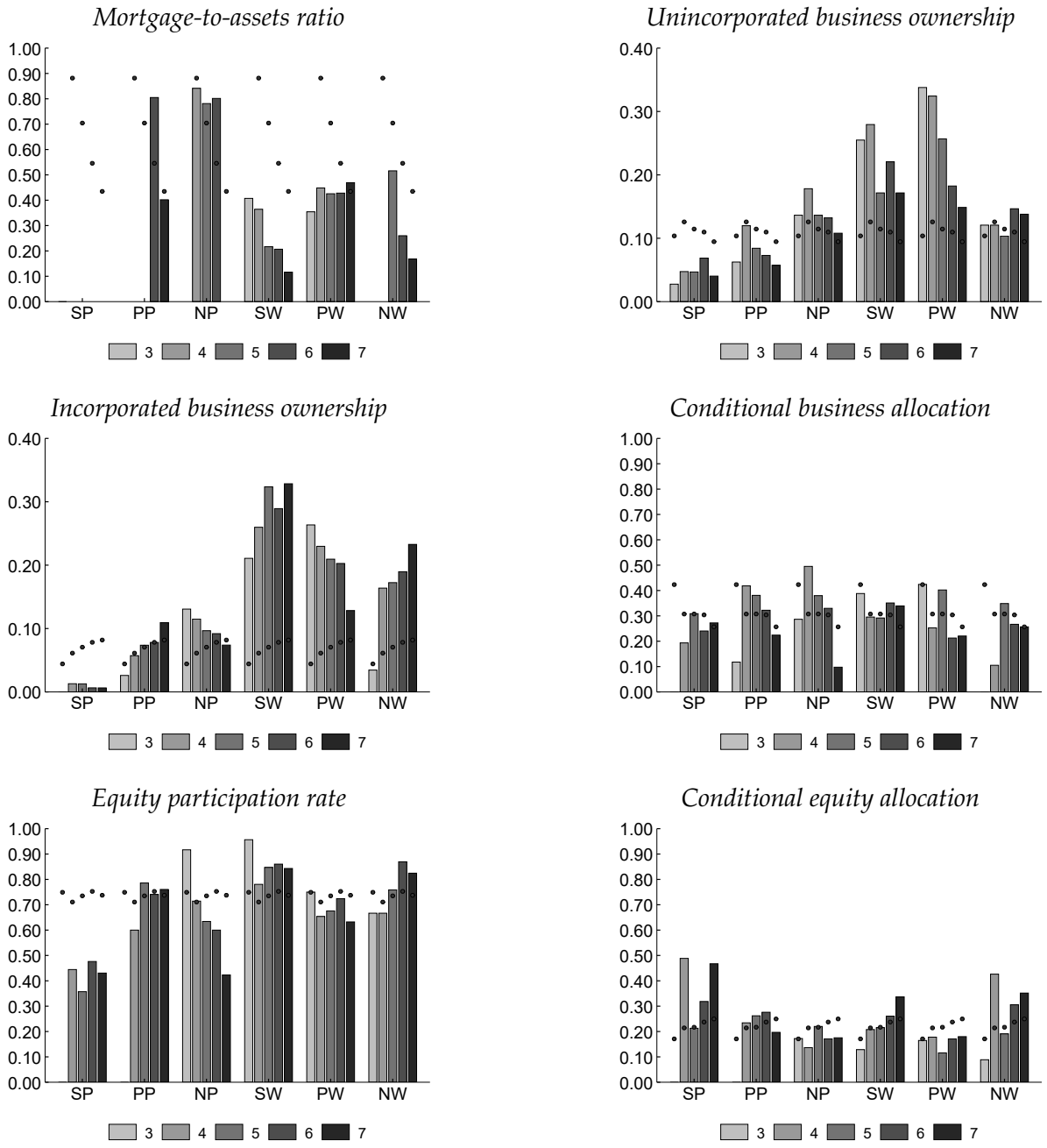

Note: Socio-economic characteristics by lifecycle stage for six discretionary groups (Section 3.4). Left column shows proportions, right column conditional medians. Section H.1 defines all metrics.

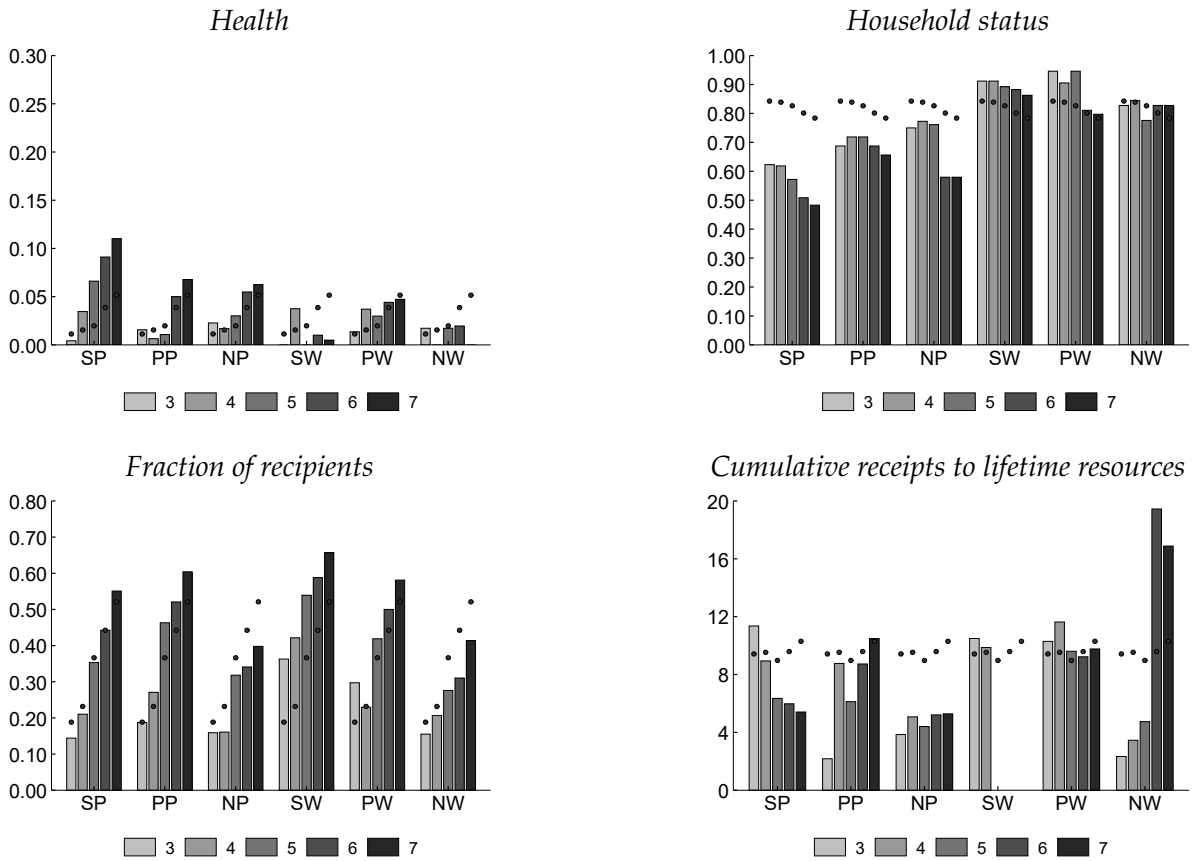

Note: Socio-economic characteristics by lifecycle stage for six discretionary groups (Section 3.4). Left column shows proportions, right column conditional medians. Section H.1 defines all metrics.